THE ASTRONOMICAL JOURNAL VOLUME 113, NUMBER 1 JANUARY 1997

MULTIWAVELENGTH OBSERVATIONS OF COLLISIONAL RING GALAXIES. I. BROAD-BAND IMAGES, GLOBAL PROPERTIES, AND RADIAL COLORS OF THE SAMPLE GALAXIES

P. N. APPLETON[1]

E. W. Fick Observatory, Department of Physics and Astronomy, Iowa State University, Ames, Iowa 50011
Electronic mail: pnapplet@iastate.edu

A. P. MARSTON[1]

Department of Physics and Astronomy, Drake University, Des Moines, Iowa 50311
Electronic mail: TM9991R@acad.drake.edu

Received 1995 November 13; revised 1996 October 3

ABSTRACT

This is one of a series of papers discussing the optical, infrared and radio continuum properties of a sample of collisional ring galaxies. The present paper concentrates on the global broad-band optical (B, V and R) and near-IR (J, H and K) images of the galaxies and describe their global properties. An analysis of the colors of the galaxies over a variety of wavelength baselines is described. In the B and V bands, the bluest colors are found in the outer bright ring. The $B-V$ colors of the sample of galaxies are blue, the mean value for the sample is $B-V=0.60$, and V-$K=2.37$ mag. The IR morphology of the galaxies is, in most cases, very similar to that of the B-band data, suggesting that the clumpy appearance of the star formation in the outer rings is real, and not a result of patchy dust obscuration. Only in one ring (WN1, a Seyfert ring galaxy) was the IR morphology different from the optical, suggesting the presence of significant dust in the disk. In II Hz 4, faint spiral arms are seen within the ring. There is a suggestion that the larger rings have redder V-K colors, which may be due to an increased incidence of nuclear bulges in larger ring galaxies. Radial profiles of surface brightness and color are presented for four galaxies. In all cases, the colors becomes bluer as one proceeds radially outwards, but in two galaxies, the rings redden again outside the main ring, suggesting the existence of a red stellar population that may have pre-dated the collisions. © *1997 American Astronomical Society.* [S0004-6256(97)01601-4]

1. INTRODUCTION

In this series of papers we examine a sample of a rare class of colliding galaxy, the collisional "ring" galaxies. The prototype of these galaxies is the beautiful "Cartwheel" galaxy, A0035-33. A review of collisional ring galaxies has recently been presented by Appleton & Struck-Marcell (1996). The dominant ring morphology is thought to result from a head-on collision between two galaxies, one of which traveled close to the spin-axis of the other, striking the disk close to its center. The resulting gravitational perturbation is believed to drive a set of symmetrical waves or caustics through the stellar disk (Lynds & Toomre 1976; Theys & Spiegel 1976; Toomre 1978; Struck-Marcell 1990).

Early, mainly photographic studies of a few ring galaxies, hinted at the existence of significant extended star formation making them appear quite blue (Cannon *et al.* 1970; Theys & Spiegel 1976). Far-IR studies of ring galaxies showed that ring galaxies are strong IR emitters with higher than normal far-IR color temperatures similar to other interacting systems (Appleton & Struck-Marcell 1987a; Wakamatsu & Nishida 1987). Ring galaxies are shown to contain copious quantities of molecular gas, although very little is yet known about its distribution (Horellou *et al.* 1995). Fosbury & Hawarden (1977) showed that the Cartwheel ring galaxy is the site of extremely vigorous star formation and this is found to be a common property of the ring galaxies (Marston & Appleton 1995; Paper II, hereafter MA).

Except for a few recent studies of individual ring systems (Higdon 1993; Schultz *et al.* 1990; Gerber & Lamb 1994; Wallin & Struck-Marcell 1994), our observations represent the first CCD study of the optical properties of a sample of ring galaxies. Aside for earlier work published by us on two of the present sample (Cartwheel–Marcum *et al.* 1992; NGC 985–Appleton & Marcum 1993) very little near-IR imaging of photometry has been performed by previous workers. Bushouse & Stanford (1992) published a K-band image of Arp 147 as part of a larger sample of interacting galaxies. Our study represents the first systematic IR study of ring systems.

In this paper (Paper I) we present a small atlas of optical and IR images of a sample of northern ring galaxies and will concentrate on their global photometric properties. For some of the larger systems we present radial color profiles of the galaxies. Paper II (MA, which was published in advance of this atlas) discussed the distribution of star formation regions in a subset of this sample, based on Hα imaging of the galaxies. In a detailed analysis in Paper III (Appleton *et al.* in

[1]Visiting Astronomer at the Kitt Peak National Laboratory Observatory. KPNO is operated by the Association of Universities for Research in Astronomy under contract with the National Science Foundation.

 0004-6256/97/113(1)/201/24/$10.00

TABLE 1. The sample galaxies.

Name (1)	Alternative Name (2)	*IRAS* Name (3)	RA(1950) h,m,s (4)	Dec(1950) deg,′,″ (5)	V(Hello) km/s (6)	Ring Type (7)
LT41	none	none	00 05 23.8	−04 50 06	21,367	RN
Cartwheel	Zwicky's Ellipse	00352−3359	00 35 14.3	−33 59 27	8,934	RN
IIIZw33	VV790a	01412+1648	01 41 14.0	+16 48 36	8,036	RE (pec)
NGC985	VV285	023221−0900	02 32 10.5	−09 00 22	12,950	RK
Arp10	VV362	02158+0525	02 15 48.8	+05 25 17	9,104	RN
IIZw28	VV[a]/90b	04590+0330	04 59 04.1	+03 30 06	8,611	RE
IIHz4	none	none	08 55 23.0	+37 16 50	12,830	RN
WN1[a]	none	09595−0755	09 59 30.9	−07 55 15	16,500	RK (pec)
VIIZw466	VV788	12297+6641	12 29 51.8	+66 40 46	14,335	RE
Abell 76[b]	P-K050-3601	21274-0301	21 27 28.8	−03 01 34	3,412	RK?
LT36	KUG2348+270	23482+2700	23 48 15.4	+27 00 35	8,002	Irr

[a]Discovered by Wakamatsu & Nishida (1987).
[b]Originally misclassified as a planetary nebula (see Talent *et al.* 1982).

preparation) we will present optical spectroscopy and detailed color information for the various star forming knots in the galaxies and compare them with model expectations of the evolution of stars behind the expanding rings.

In Sec. 2 we discuss the sample of ring galaxies. The observations and data reduction is described in Sec. 3. In Sec. 4 we present an atlas of images and in Sec. 5 the integrated properties of the galaxies. Radial color information for four of the larger galaxies is presented in Sec. 6 and the conclusions are given in Sec. 7.

We assume throughout the paper a value for the Hubble constant of 75 km s^{-1} Mpc^{-1}.

2. THE SAMPLE

In Table 1 we present information about 11 mainly northern ring galaxies or ring-like galaxies which were selected primarily from the list compiled by Appleton & Struck-Marcell (1987a) from the literature. Since our aim was to study the properties of rings as a function of their collisional ages and different possible collisional impact parameters, an attempt was made to select galaxies with a range of linear sizes and ring types. The ring galaxies have radial velocities ranging from 3412 to 21 367 km s^{-1}. In terms of linear scale they range from rings with diameters of as little as 2 kpc, to the large rings of the Cartwheel and NGC 985 with ring diameters of 30 kpc. The sample is necessarily ad-hoc for a number of reasons. The space density of ring galaxies is rather low (see Appleton & Struck-Marcell 1996). Hence ring galaxies are relatively distant faint objects, and no complete catalog exists for them in the North (the situation in the southern hemisphere is a little better, due mainly to the work of Few & Madore (1986) and the construction of the Arp-Madore Atlas of Southern Galaxies and Associations (Arp & Madore 1987)). The only systematic study of ring galaxies made in the north is that of Thompson (1977) who searched photographic plates for ring galaxies near clusters. However, many of the galaxies in his list are extremely small, and several do not have well determined morphologies and may not be collisional ring systems. We included two of the larger galaxies in Thompson's list, LT 36 and LT 41, in our study here.

The first systematic classification of possible collisional rings was devised in the observational paper of Theys & Spiegel (1976). These authors classified rings into three loose categories which we shall use for convenience here in describing our sample. The three types are RE (empty rings), RN (which have nuclei in or near the ring center), and RK (ring galaxies with a bright knot in the ring which breaks its symmetry). Our sample of ring galaxies, presented in Table 1, contains rings representative of each Theys & Spiegel class (4 RNs, 3RKs, 3REs, and 1 irregular rings). All of the sample members are accessible from the northern hemisphere, although a number are best observed at low latitudes. Cartwheel data has been obtained from Mauna Kea Hawaii with supplementary data from J. Higdon (ATNF). We note that the classical empty ring galaxy Arp 147 was not included in our survey because it has been studied in detail elsewhere (e.g., Bushouse & Stanford 1992; Schultz *et al.* 1990; Gerber & Lamb 1994; Mazzei *et al.* 1995; McCain 1996). With this exception, the galaxies contained in our sample include most of the well known northern ring galaxies.

Although we have attempted to restrict our study to a sample of what we hope are truly colliding systems, we discovered, during our study that two of the galaxies (LT 36 and Arp 10) are probably not classical ring systems, despite their appearance on photographic plates. Collisional ring galaxies are generally thought to form a distinct class which differ morphologically from ringed or pseudo-ring galaxies (see, for example, Buta 1986) by virtue of the lack of obvious inner stellar bar or lens component. In the pseudo-ring galaxies, the nucleus is usually central to the ring, whereas in RN collisional systems, this is usually not the case. Collisional systems also have a companion galaxies somewhere close to the minor axis of the ring. (See Theys & Spiegel 1976; Athanassoula & Bosma 1985; Buta 1986.) Arp 10 was first thought to be a classical ring because of its bright blue ring and a small companion near the minor axis (Charmandaris *et al.* 1993). However, recent HI and optical observations suggest that it may be an example of two galaxies in a more advanced stage of merger (Charmandaris & Appleton (1996)). Likewise LT 36, from the observations presented here, is not a clear example of a collisional ring, although

there are definite signs of a recent interaction. Despite these differences, we include for completeness data on these ring-like systems here.

3. THE OBSERVATIONS

The observations described here fall into two categories. Firstly, optical CCD images were made with the 2.1-meter telescope at the Kitt Peak National Observatory (KPNO) and the 0.6-meter telescope at the Erwin W. Fick Observatory of Iowa State University. Secondly, near infrared observations were made with the 2.1-meter KPNO telescope and for two galaxies (The "Cartwheel" galaxy and NGC 985) observations were obtained with the 3.8-meter UKIRT. A complete description of the latter observations is presented in Marcum *et al.* (1992); hereafter MAH, and Appleton & Marcum (1993) and only the global properties will be discussed here. The majority of the optical CCD observations were made with the KPNO 2.1 m telescope with a TEK-2 512×512 CCD detector on the nights of 1992 January 16, 18, and 19 under photometric conditions and average (2″–3″) seeing. Broad-band Johnson-Harris B and V observation were made with a plate-scale of 0.34″ per pixel. After experiencing some difficulties with flat fields for the Johnson/Harris R filter early in the first night of observation, the R filter was replaced with a "Nearly-Mould R" (NM) filter for the remainder of the observing. Except for one galaxy (II Zw 28) all of the other galaxies were observed with the NM filter. Based on observations of various standard stars and observations of II Zw 28 through both filters, we have determined that only a small correction was required to convert NM filter onto the Harris R magnitude scale. (We determined that $m(R)_{\rm Harris} = m(R)_{NM} - 0.12$ with a negligible color term over the range of $V-R$ colors of interest here.) All magnitudes in this paper are therefore on the Johnson/Harris BVR system.

Observations of two of the sample galaxies were carried out in the optical with the Fick Observatory wide-field CCD system (see, for example, Appleton Kawaler & Eitter 1993 or Charmandaris *et al.* 1993; hereafter CAM). The 0.6 m Mather telescope combined with a focal reduction system provides an $f/4$ beam at the Cassagrain focus, and the unvignetted field of view is 16×16 arcmin^2 at the detector. The detector used was a TI 800×800 CCD, providing a 1.35″/pixel plate scale. Broad-band BVR (Harris) observations of Abell 76 were made on 1992 October 1 and 2 and those of NGC 985 were made on 1993 October 12 and 22. On all three occasions the observations were made under good conditions of transparency and seeing (for the observations of NGC 985 the seeing was close to the size of a single pixel—1.35 arcsecs). Conditions were photometric during these observing periods. Calibration was achieved using the standard stars 92-263 and 113-466 (Landolt 1992).

The infrared observations were made during two observing runs on the nights of 1990 November 4–7 and 1991 July 25–27 with the IRIS 58×62 element photovoltaic array camera attached to the KPNO 2.1-meter telescope. The plate scale was 0.73 arcsec/pixel and the field-of-view of the array was 42.3×45.3 arcsecs. The conditions were excellent and the seeing was 1–2 arcsecs during most of the observing runs. Observations were made of both the object and adjacent regions of blank sky. The raw images were first dark subtracted and flat fielded using standard analysis methods (see, for example, Appleton *et al.* 1992). The sky frames obtained during observations were median averaged and normalized to provide a local flat-field for the object frames. The observations were then calibrated using the following IR standard stars obtained from the list of Ellias *et al.* (1982): HD 1160, 3029, 162208, 18881, 201941, 203856, 22686, 44612, and GL 299, 748, and 811.1. The observations and data reduction for the UKIRT observations of the Cartwheel and NGC 985 are discussed fully by MAH, and Appleton & Marcum (1993).

4. ATLAS OF THE GALAXIES

In this section we discuss the galaxies individually and present grey-scale and contour maps of a subset of the imaging data.

In Figs. 1 to 11 we present contour maps and images of ten out of eleven of the sample galaxies. In each figure we present where possible, the B, R, and K contour maps and the V- or R-band image in grey-scale form. In most cases we have attempted to include the companion galaxy in the figures. In some cases (for example, VII Zw 466) additional IR maps are presented because of interesting spectral properties of some of the knots. We provide below a very brief summary of each galaxy. Images of the some of the sample have been presented elsewhere and will not be repeated here (near-IR and optical images of the Cartwheel, see MAH, optical images: Higdon 1993; near-IR images of NGC 985, Appleton & Marcum 1993). We note that Hα and K-band grey-scale images were presented of the sample in MA.

4.1 LT41

This galaxy is from the list of Thompson (1977). It is a fine example of a collisional ring system (Fig. 1). The elliptical companion lies on the minor axis and the galaxy shows a typically strong asymmetric distribution of emission at almost all bands. Jeske (1986) in his Ph.D. thesis, reported uncalibrated CCD images and some spectra of this galaxy. Except for this unpublished thesis work, no previous work has been reported on this galaxy (see Paper II for a discussion of the star formation distribution). The central bulge of the ring galaxy is typically offset from the geometrical center of the ring in a manner similar to the Cartwheel. Unlike the Cartwheel, no evidence is found for strong spokes between the ring and the central regions. The brightest knots lie along the southern edge of the ring and this asymmetry, typical of many ring galaxies, is also seen in the K-band image. The striking similarity between the B and K images suggests that absorption by dust in the ring is minimal. This is the highest redshift ring in the sample ($z = 0.074$). In Sec. 6 we present evidence for strong radial color gradients in the galaxy. However, the existence of a small, high surface brightness bulge makes the interpretation of the color gradient in term of stellar evolution behind the ring wave ambiguous.

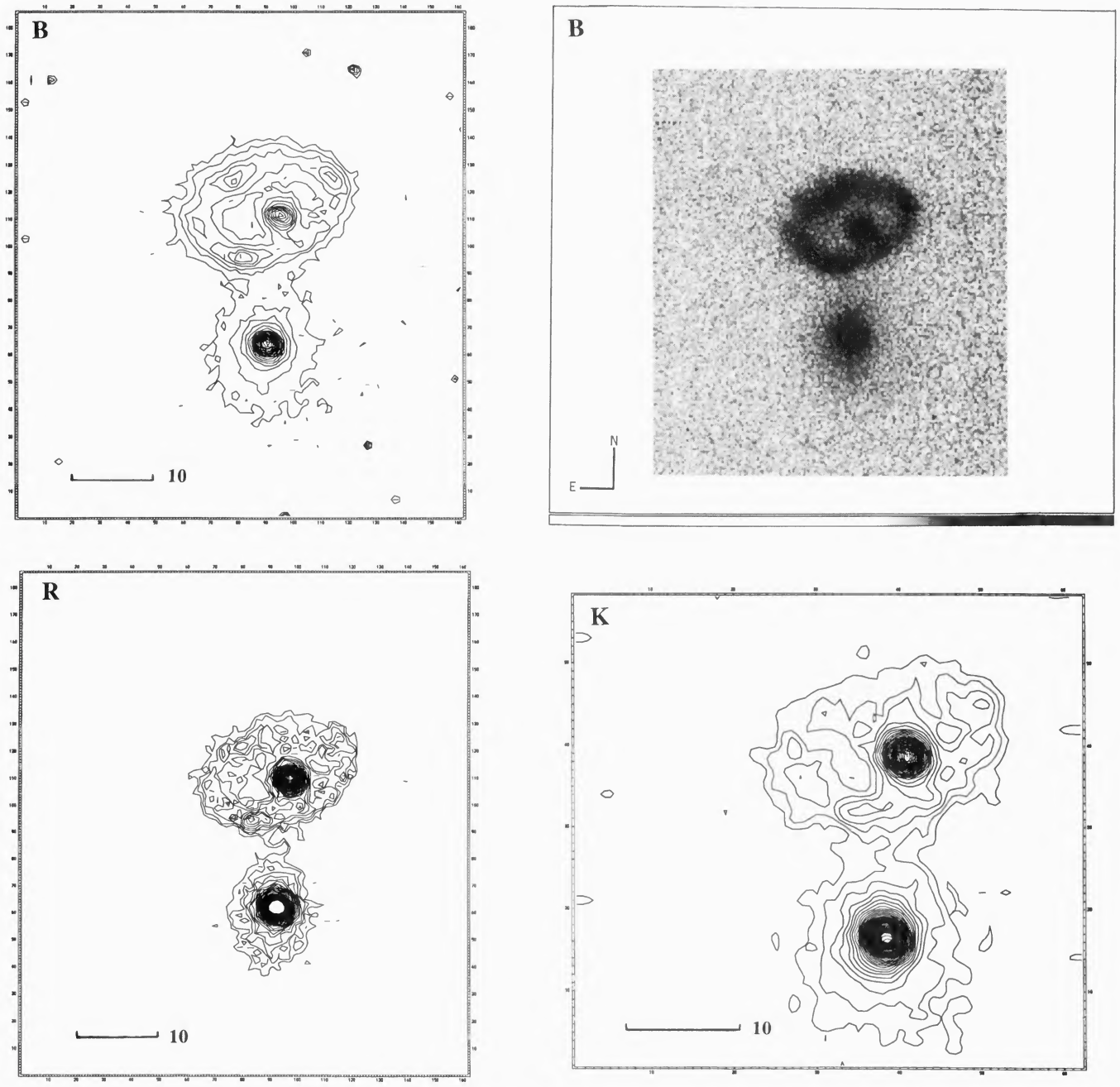

FIG. 1. Contour maps and grey-scale images of LT 41 in B, R, and K-band light. The bar indicates the image scale in arcsecs (as with Figs. 2–11).

4.2 II Zw 28

This interesting galaxy is one of the few empty ring galaxies without an obvious massive companion (Fig. 2). It was first discussed by Sargent (1977) because of its notably strong Balmer absorption lines suggesting a large population of A-stars. The ring itself is extremely asymmetric, forming a crescent shape. Faint emission fills the disk. We show evidence for at least one small galaxy (see R-band image) a few diameters away from II Zw 28 to the NW. The R- and K-band image emphasizes the boxy nature of the bright region of the crescent. This is due either to the bulge of the original target galaxy which has been displaced from the ring center or may be due to a companion galaxy seen in projection against the ring. The galaxy is one of the few *not* detected in a recent sensitive CO survey of ring galaxies (Horellou *et al.* 1995).

4.3 VII Zw 466

This ring galaxy is a classical empty ring (type RE) in a small group (Fig. 3). The ring is not really empty and in Appleton & Struck-Marcell (1996) we preferred to describe these RE rings as ''centrally smooth'' since they contain mainly red light. The Hα emission-line properties are discussed in MA. A comparison between the B- and K-band images shows again a remarkable similarity. The brightest knots seen in the B-band image are also the brightest knots at

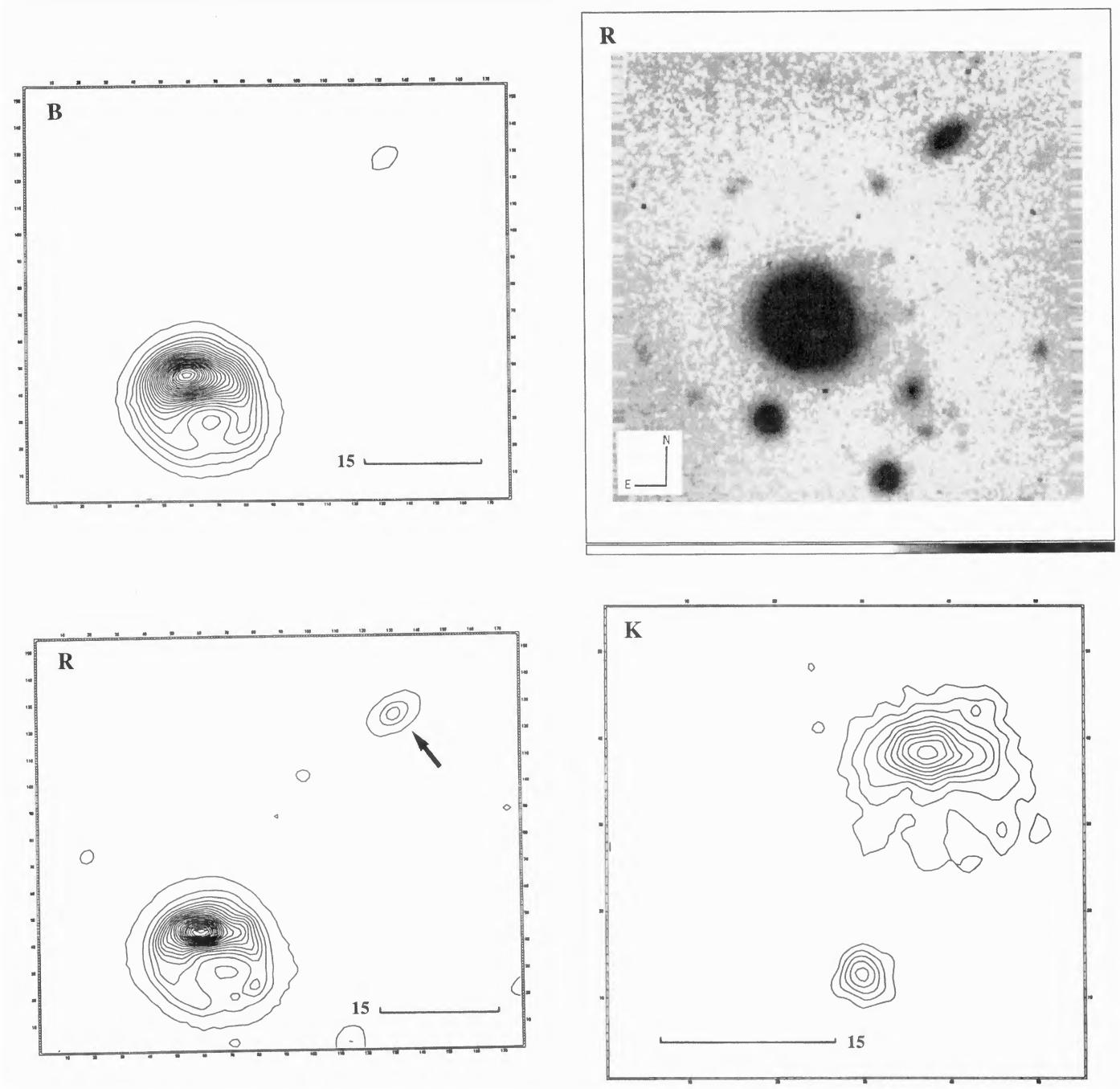

FIG. 2. Contour maps and a grey-scale image of II Zw 28 in B, R, and K-band light. Note the possible companion in the lower R-band contour map (arrow).

K-band. It had been suggested by Toomre (see Thompson & Theys 1978) that the knot seen interior to the ring at a P.A. of 275° might be the displaced nucleus of VII Zw 466. This seems very unlikely, since the knot is rather weak at K-band (it is however slightly brighter at J-band; see Fig. 3). We believe that this knot is indistinguishable from the other star forming regions in the ring and is unlikely to be a displaced nucleus. There is a hint in the B-image, that it lies on a circular bubble-like structure, and we suggest that it represents a regions of secondary star formation resulting, perhaps, from the formation of a large super-shell centered on a previous region of massive star formation.

The three possible companions are shown in Fig. 3. The peculiar elliptical galaxy G1 has ''boxy,'' slightly asymmetric, outer isophotes, suggesting perhaps that it was the ''intruder'' galaxy that created the ring. However, recent H I observations by Appleton *et al.* (1996) show that the edge-on disk G2 is more likely to have been the intruder galaxy. Galaxy G2 has an unusually blue knot on the side of the galaxy which points back towards VII Zw 466 (see B and R images). Galaxy B1 is a background galaxy (R. Lynds, see discussion by Theys & Spiegel 1976), a result confirmed by recent optical spectroscopy.

4.4 II Herzog 4 (II Hz 4)

This is the classical ring galaxy that was modeled so elegantly by Lynds & Toomre (1976). The observations (Fig.

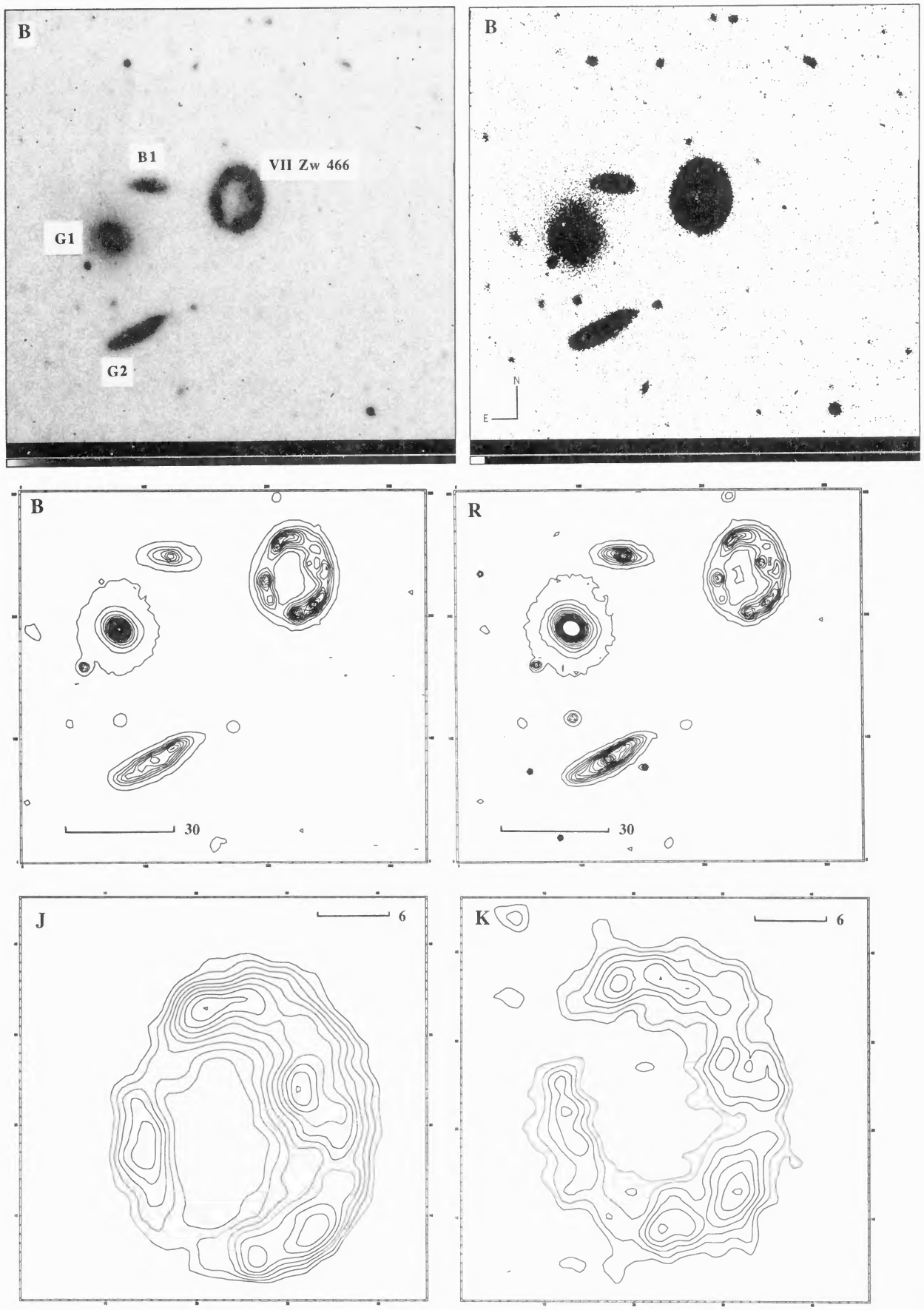

FIG. 3. Two grey-scale representations of the VII Zw 466 group and B, R, J and K contour maps of some of the galaxies. The galaxy labelled B1 is conclusively found to be a background galaxy. G1 and G2 are galaxies in the group. Evidence from H I observations strongly suggests G2 is the intruder object despite the peculiar outer isophotes G1 seen in the second grey-scale panel.

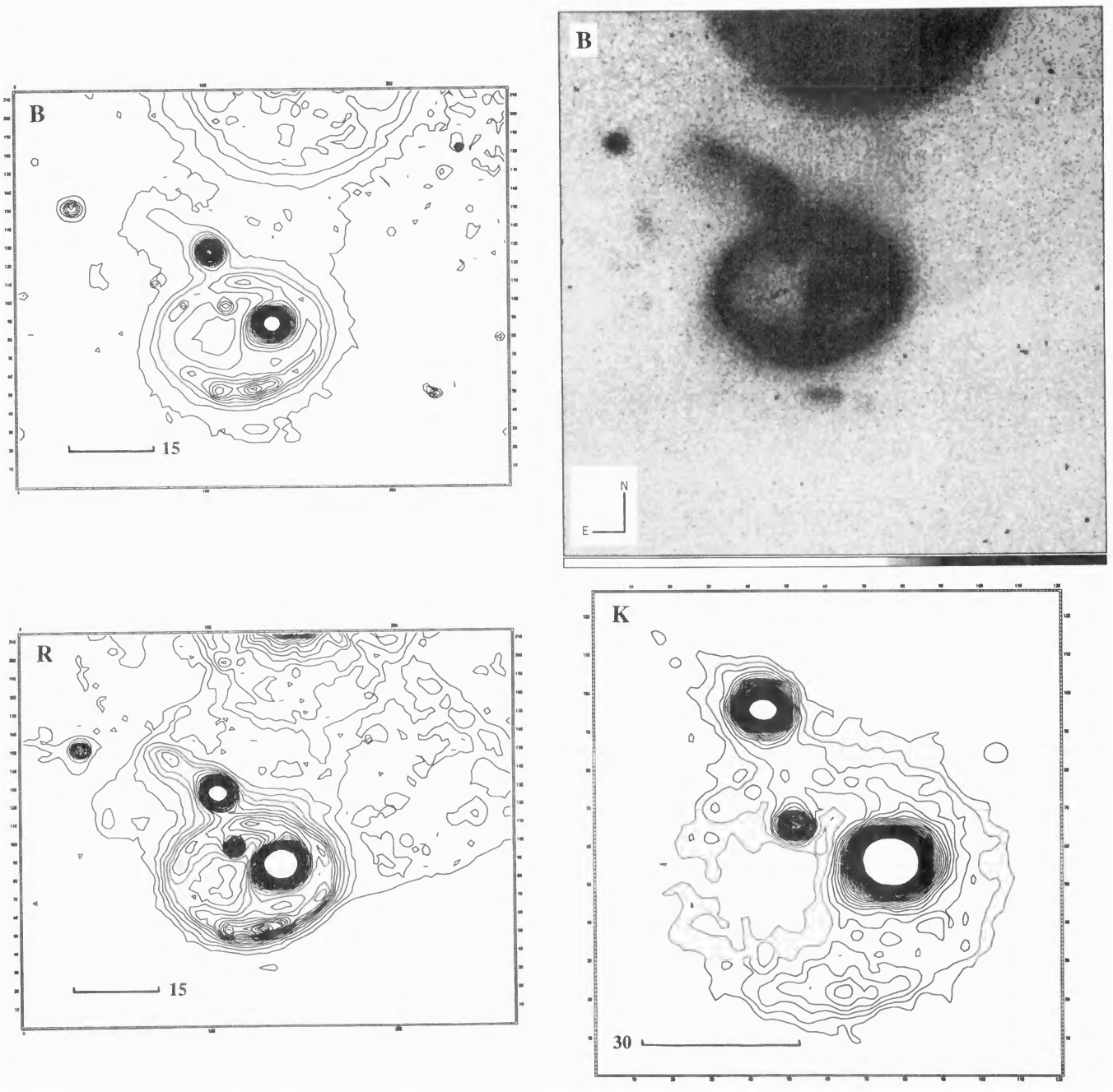

FIG. 4. B, R, and K-band contour maps and grey-scale images of the possible double-ring galaxy II Hz 4.

4) show a blue object (perhaps a dwarf galaxy) to the south of the rather knotty ring. More scattered material is seen to the east of the ring just south of the tail of the companion. The off-set nucleus of the ring shows two spiral arms. In order to show the existence of the arms more clearly, we show in Fig. 5 the appearance of the galaxy after subtracting a symmetrical Gaussian from the nuclear regions. Two arms connected to a slightly elongated bulge can be seen. The northern arm appears to connect to the ring in the north. The arms are rather unlike the Cartwheel spokes and are more likely some form of stellar resonance (see Appleton & James 1990, for a discussion of similar arms in AM 064-741). Again, very little difference is seen in the K-band and B-band images, regarding the bright knots in the ring.

The galaxy lies very close to a bright star (on northern edge of Fig. 4) which complicates our interpretation of the possible second ring which allegedly is seen to the north of the companion nucleus (Lynds & Toomre 1976). Given the scattered light from the star at all wavelengths we were unable to confirm the reality of the second ring. Unfortunately, the star was so bright that its effects, especially in the red, were enormous. In addition, a diffraction spike extends from the star towards the galaxy in the optical wavebands, giving the impression of a connection with the galaxy and possible continuity of the northern plume from the companion into a ring. However, the 4-meter photographic plate presented by Lynds & Toomre (1976) seems to convincingly show a second ring. We note that the tidal tail to the companion galaxy is very blue and has very little emission at either R or K band. In Sec. 6, we present radial color profiles of the galaxy

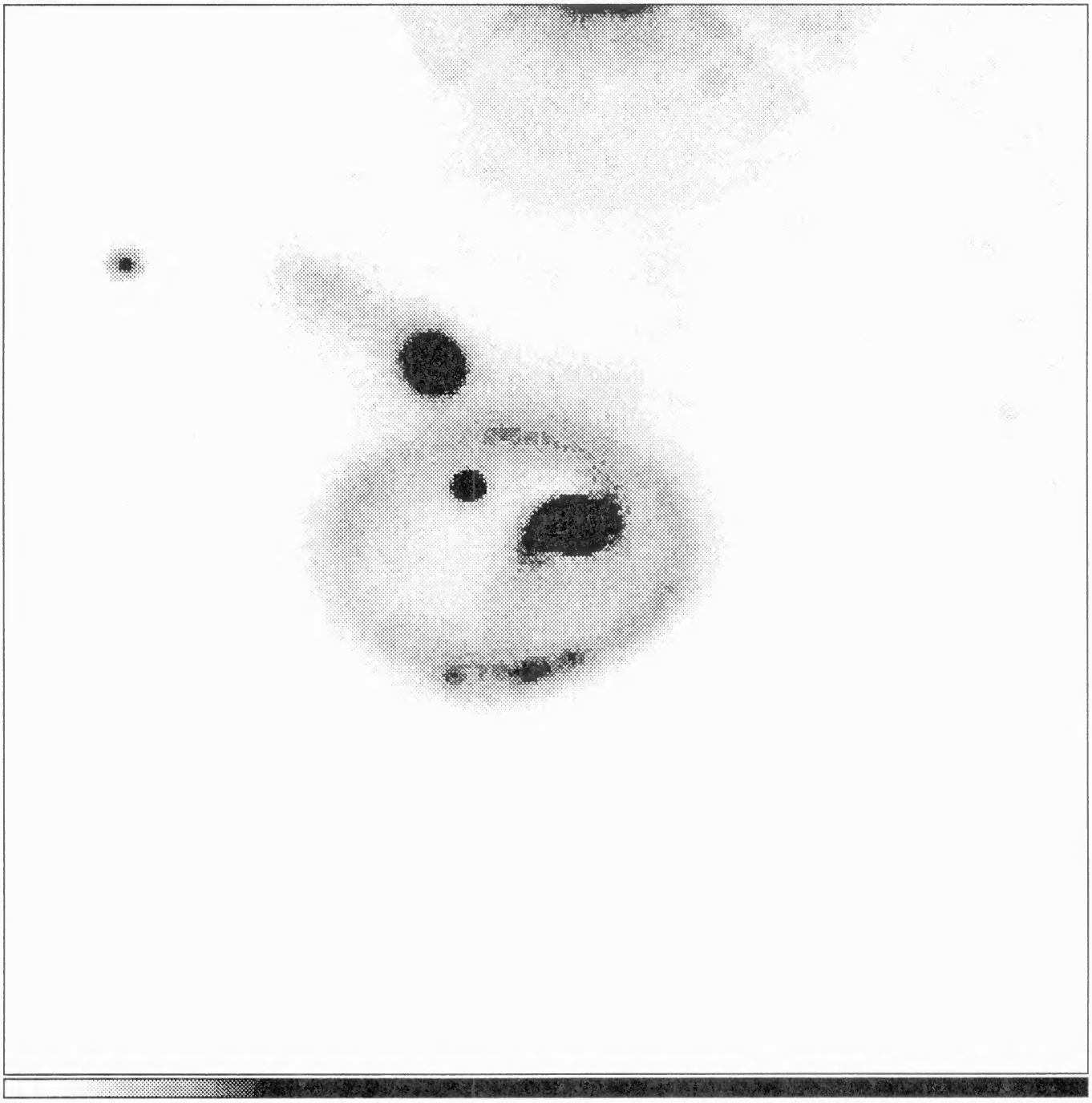

FIG. 5. Grey-scale *R*-band Image of II Hz 4, emphasizing the 2-armed spiral in the inner regions of the galaxy (see text).

after the removal of the foreground starlight from the image using software.

4.5 WN1 in Bootes

This Seyfert 1 galaxy was discovered by Wakamatsu & Nishida (1987), hereafter called WN1. The ring is very asymmetric (Fig. 6) and has the appearance of a bow-shock structure and appears to be a classical example of an offset collision forming a ''banana-type'' wave (see Appleton & Struck-Marcell 1987b). A highly elongated companion galaxy is seen to the north-west of the nucleus. This galaxy strongly emits radiation from CO molecular lines (Horellou *et al.* 1995). A brief discussion of the near-IR properties was made by Appleton *et al.* (1990). The Seyfert nucleus dominates the emission from the nucleus at all wavelengths. This galaxy, unlike most of the other ring systems presented in this paper, shows significant color differences when the optical-IR baseline is considered. The most dramatic difference is in the appearance of the companion galaxy which appears as a normal edge-on galaxy at IR wavelengths (see *K*-band image). However, at optical wavelengths, the nucleus appears to be masked by the disk of the ring and the brightest emission at *B*-band comes from the very tip of the

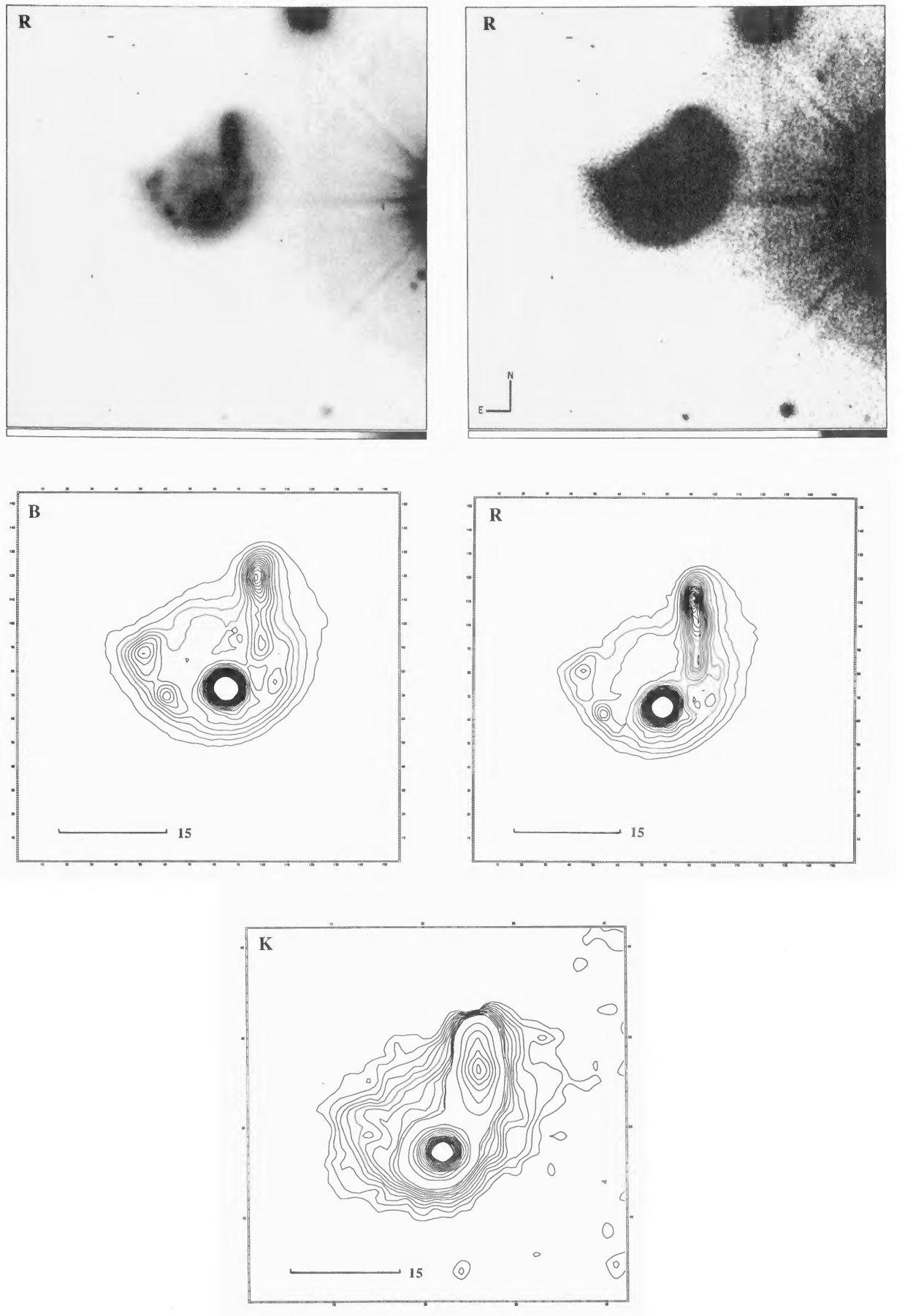

FIG. 6. Grey-scale images and contour maps at B, R, and K-band of the Seyfert ring galaxy WN1. Note the peculiar sharp outline of the galaxy at faint levels (panel 2) and the significant differences between the companion galaxy morphology at optical and near-IR wavelengths (see text).

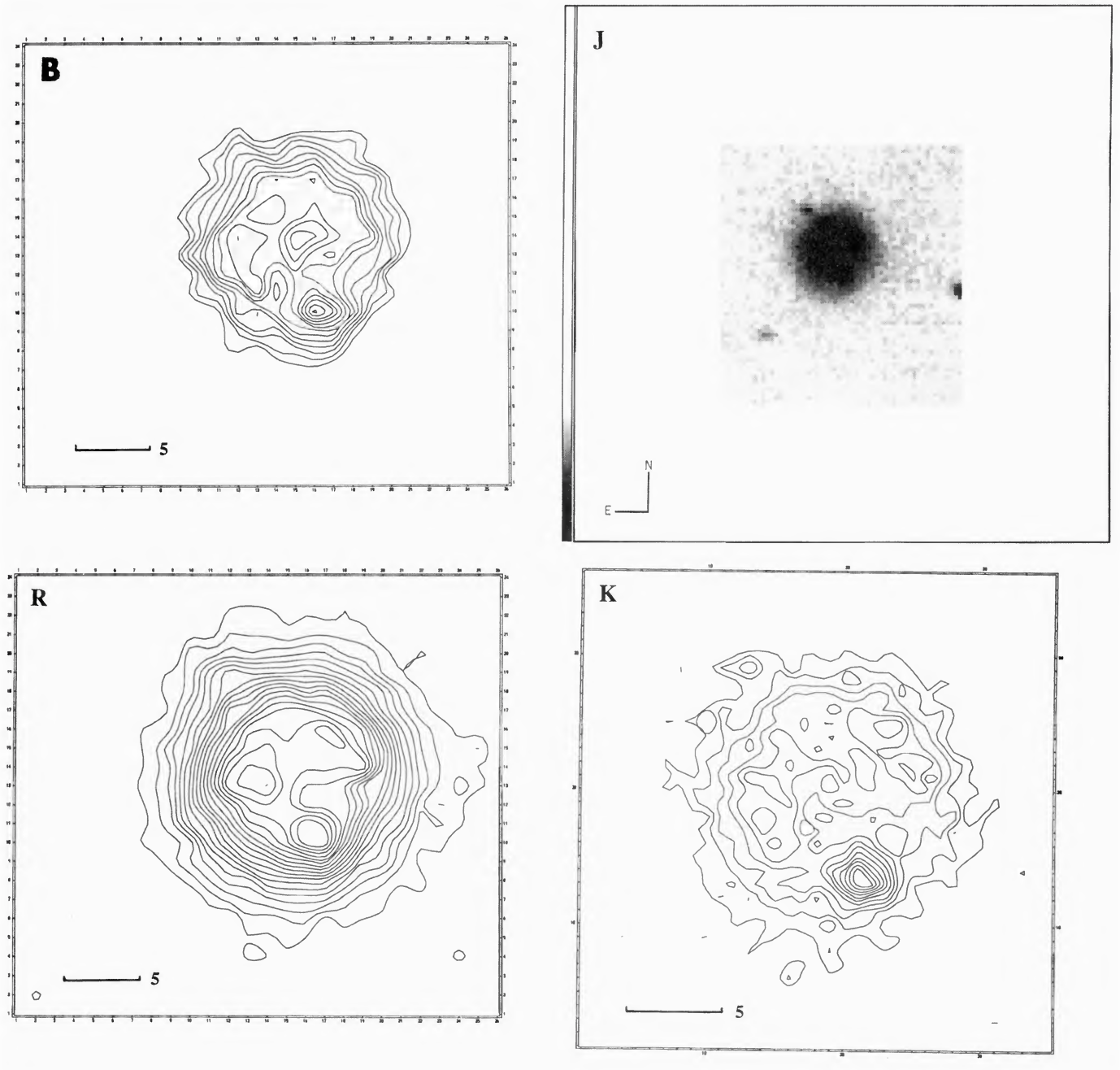

FIG. 7. *B*, *R*, and *K*-band contour maps and grey-scale images of Abell 76.

companion's disk. This strongly suggests that the companion galaxy lies behind the disk of WN1 and that the absorbing medium contains a significant amount of dust. Other optical-IR differences are also apparent in the images. The disk of WN1 (which is quite extensive at optical wavelengths; see Fig. 6: third and fourth panels) is almost absent at *K*-band. Also the three bright star-forming knots which form the leading-edge of the bow-shock structure are not equally represented at *K*-band. The knot to the north-east is significantly weaker at *K*-band than at *B*. The *B*-image shown in Fig. 6 (second panel) shows the very strange sharp-edged morphology of the outer disk. Such sharp linear features are typical of strong tidally generated "caustic edges" (see Struck-Marcell 1990).

4.6 Abell(pn) 76 (= FIRAS 21274-0301)

This galaxy (Fig. 7), originally classified as a planetary nebula, was determined to be extragalactic by Talent *et al.* (1982) who classified it as a collisional ring galaxy. The IR images, which were of higher resolution than the optical images, show an irregular edge-brightened morphology. The companion may be the brighter knot seen at the southern edge of the disk/ring. Recent Hα observations made during conditions of good optical seeing (Bransford & Marston, private communication) strongly support the view Abell 76 is a classical ring galaxy. It is the smallest ring in our sample, having a linear diameter of only 2 kpc for an assumed value for H_0 of 75 km s^{-1} Mpc^{-1}.

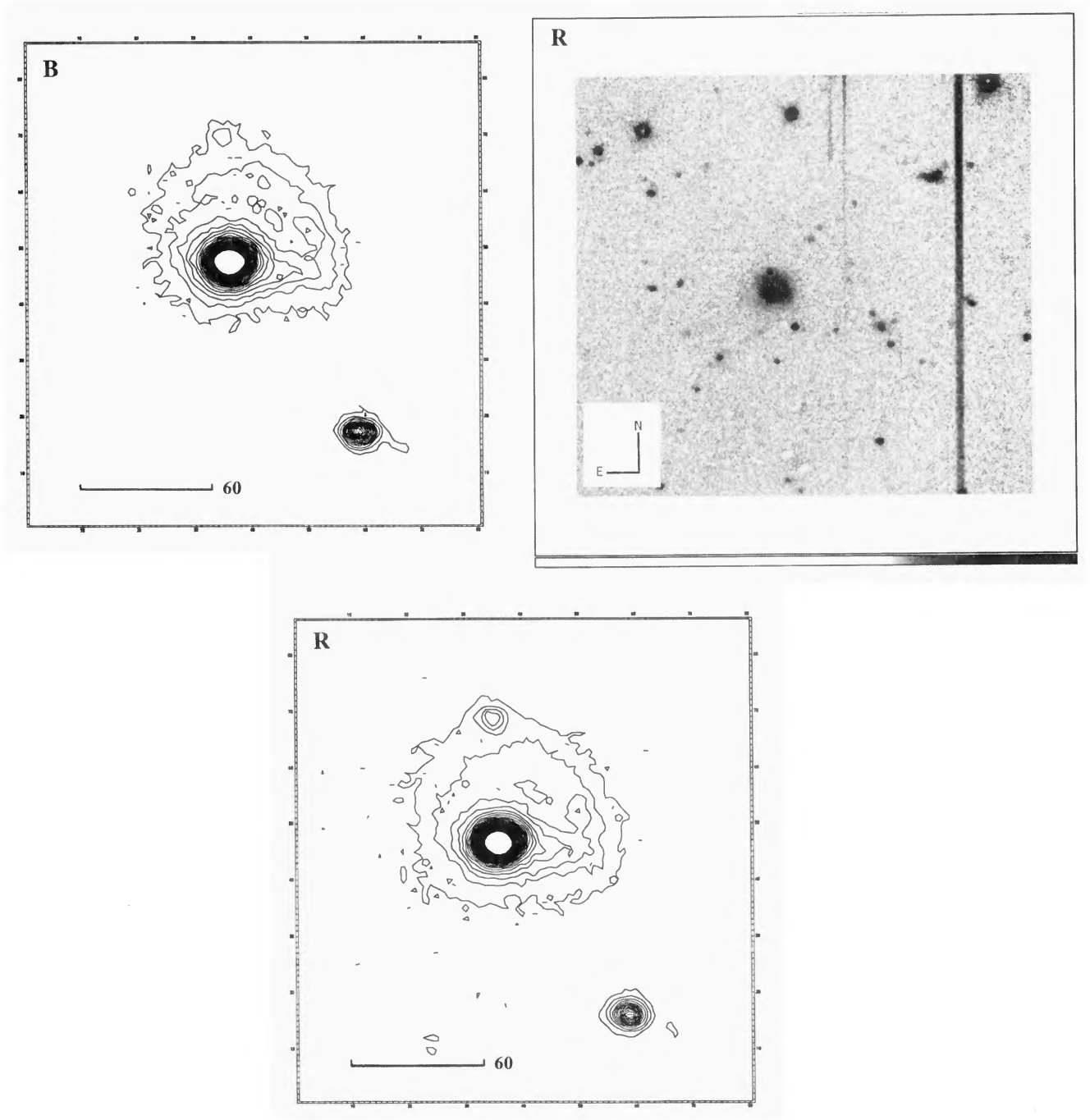

FIG. 8. *B* and *R*-band contour maps and images of NGC 985 (for IR imaging, see Appleton & Marcum 1993).

4.7 NGC 985

We present Fig. 8 optical images only of NGC 985, since the near-IR images of the galaxy are discussed in detail by Appleton & Marcum (1993). The images, taken with the E. W. Fick observatory CCD camera show the galaxy and its immediate environment. The most prominent feature aside from the bright core, which lies on the southern edge of the ring, is the ''arm'' which extends from the ring to the west. The ring itself is defined by a series of blue star forming knots. Radio observations by Appleton & Ghigo (in preparation) confirm the earlier suggestions (Rodriguez-Espinosa & Stanga 1990; Appleton & Marcum 1993) that the galaxy contains a double nucleus. As discussed by Appleton & Marcum (1993), it is quite likely that the offset bulge component, which has an $R_{1/4}$ luminosity profile, is part of the intruder galaxy seem projected against the ring. These authors showed that there appears to be two nuclei in NGC 985, again supporting the view that it is a composite system.

4.8 III Zw 33 (The ''Teardrop'' Galaxy)

This galaxy was thought to be a possible ring galaxy by Theys & Spiegel. Our observations (Fig. 9) show an irregular system with a possible faint ring and extremely bright knot embedded in it to the north-east. The main nucleus of the system is certainly off-set from any possible faint ring structure. Figure 9 shows that, at the faintest blue isophotal levels,

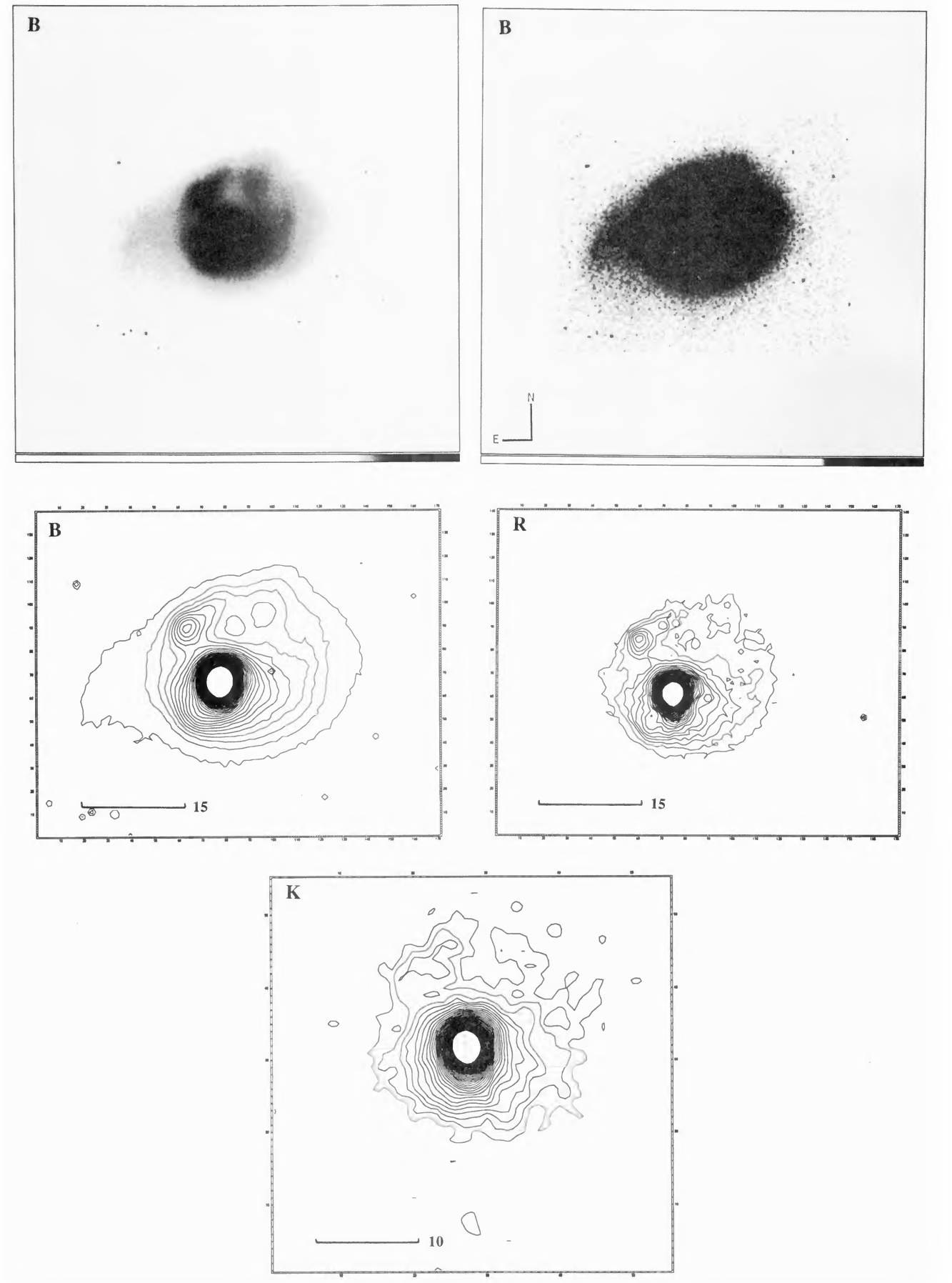

FIG. 9. *B*, *R*, and *K*-band images of III Zw 33 (the "Teardrop" galaxy). Notice the peculiar "teardrop" morphology at low levels, indicating possible evidence for tidal debris.

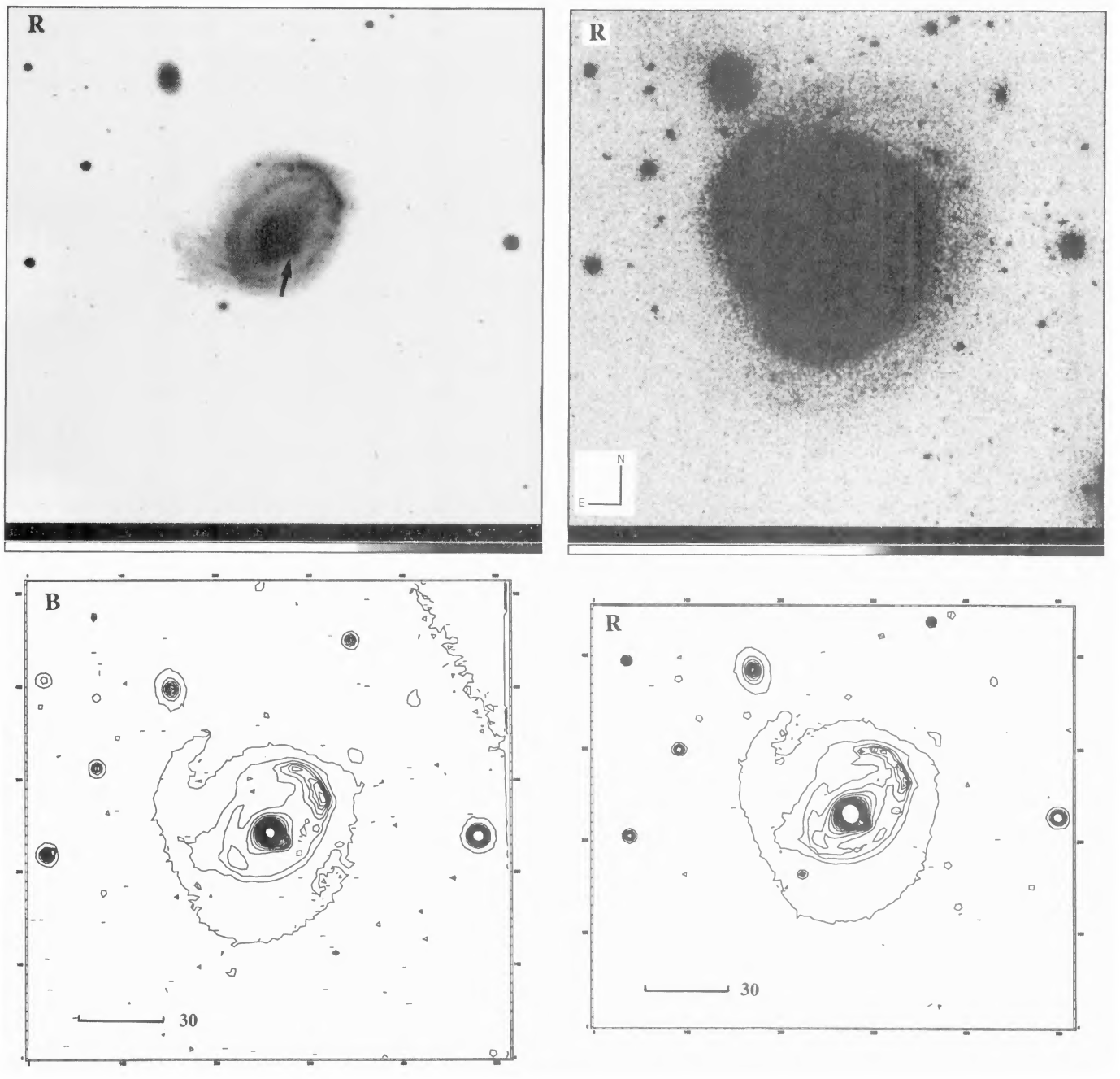

FIG. 10. The galaxy Arp 10, at *B* and *R*-band. This galaxy exhibits both bright rings and faint optical ripples. The small elliptical galaxy seen on the minor axis is a background galaxy (see Charmandaris & Appleton 1996).

the galaxy is extremely peculiar, showing a ''teardrop'' morphology. A very faint plume extends to the east of the system, perhaps indicating a violent history for the galaxy. If III Zw 33 is indeed a ring system, its companion may have been badly disrupted, producing the faint emission. It is possible that the bright knot in the ring is the remains of the nucleus of a merging second galaxy. Figure 9 supports this interpretation, since a sharp edge is seen in the lower isophotes in the northern regions, perhaps suggesting the remnants of a faint edge-on disk. Kinematic observations would allow this possibility to be tested. The IR morphology of III Zw 33 is very similar to its optical morphology.

4.9 Arp 10

Initially thought to be a classical ring galaxy by CAM, Fig. 10 shows a number of different grey-scale representations of Arp 10 to emphasize different features. Of note are the extremely bright blue knots in the north-eastern quadrant of the ring which were discussed by CAM. The bright extranuclear knot may be the nucleus of the second object since it shows Hα emission at a similar redshift to the main optical ring (CAM). Charmandaris & Appleton (1996) have shown that the elliptical galaxy, at first thought to be the companion, is in fact a background galaxy. Faint ''ripples'' are seen at very faint levels around the galaxy. These ripples compli-

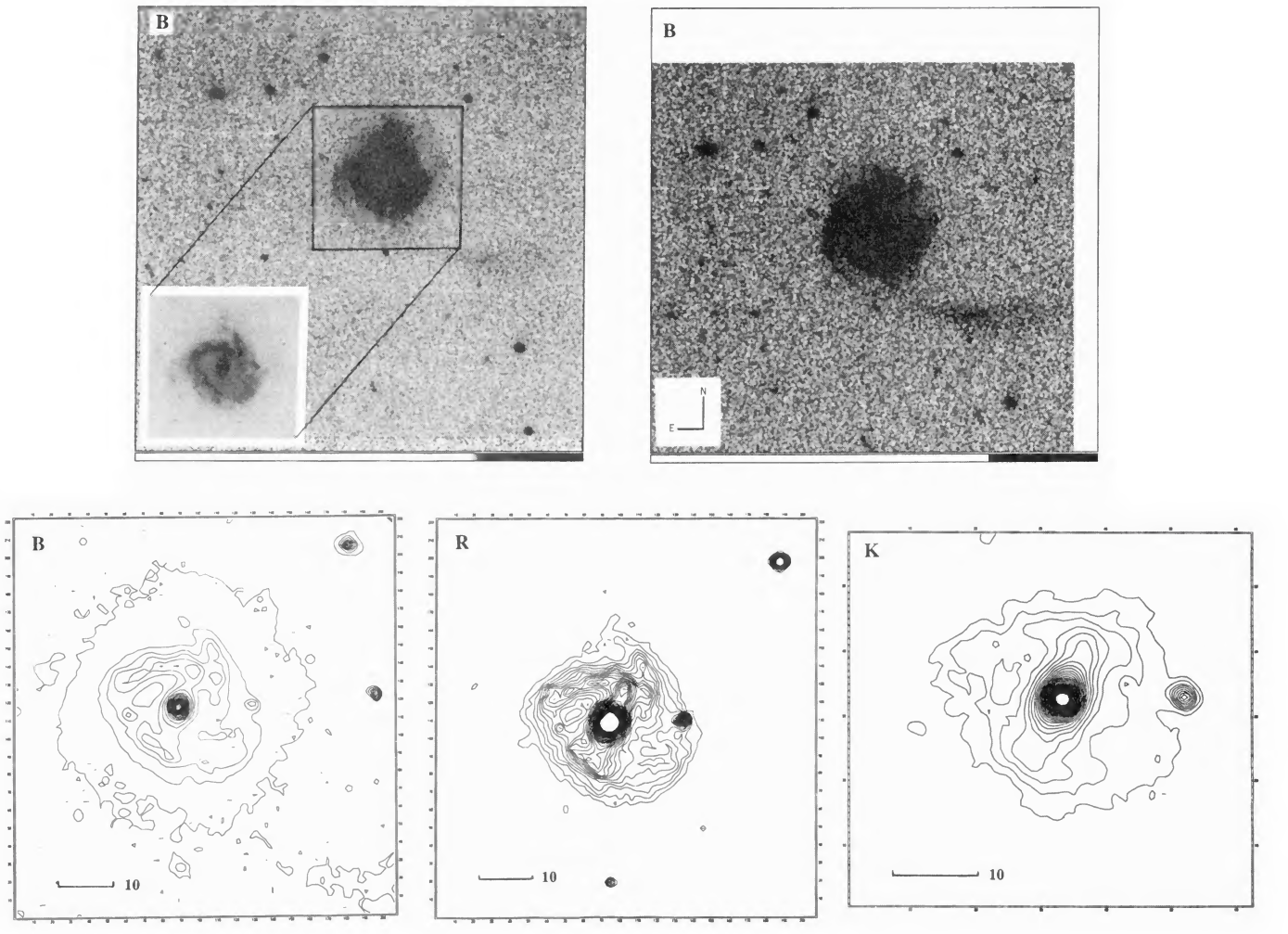

FIG. 11. The galaxy LT 36, at B, R, and K-band. Note the faint optical ripples and the possible tidal plume seen on the blue image.

cate the simple interpretation of Arp 10 as a collisional ring. Recent H I observations by Charmandaris & Appleton (1996) show that the bright inner ring is surrounded by an H I disk which extends beyond the faint "ripples." Although not as simple as ring galaxies like VII Zw 466, Charmandaris and Appleton suggest that the process that formed the rings and shells involved a central collision between a gas-poor early type galaxy and a large-type H I rich disk.

4.10 LT 36: A Possible Merger Remnant

This galaxy is also probably not a classical ring galaxy. The brightest isophotal levels of the optical and IR images (Fig. 11) show a very peculiar "theta-shaped" system, with a faint bar (which is quite prominent in the IR) and peculiar filaments extending from the ends of the bar. The galaxy shows intense star formation in the regions of the closed portion of the theta-shape. With the exception of the Seyfert rings, this galaxy is one of the few in the sample which showed Hα emission in its nucleus. The most remarkable feature of this galaxy is the huge plume and ripples in the outer regions of the galaxy seen in the blue at low isophotal levels. This suggests that the system is a merger remnant like NGC 7252 (the so-called "Atoms for Peace" galaxy of Whitmore *et al.* 1993). We are unaware of any major companion near LT 36, and so if the plume and ripples are part of the debris of a highly disrupted companion, there is no sign of the nucleus of the accreted object.

5. INTEGRATED PROPERTIES

In Tables 2 and 3 we present the photometric properties of the ring galaxies in broad-band B, V, R, J, H, K filters based on the observations. Since this paper is intended as an atlas of the images, we present here only the global photometric properties of the galaxies making only a simple decomposition of the systems into: (a) total ring galaxy emission—Table 2, (b) Ring minus interior emission—Table 3 (including any disk and bulge inside the inner edge of the ring as defined by the usually sharp fall off in light behind the outer ring), and (c) companion emission—Table 4. Although this decomposition may seem an oversimplification, we discuss our rather conservative approach below. In Paper III, we will present photometry and optical spectroscopy of individual star forming knots isolated from the images in order to discuss the detailed star formation history of emission features both in the outer ring and within the radius of the rings.

Because a number of the rings discussed in this paper contain bulges, it is likely that the bulge light dominates the

TABLE 2. Global optical and IR photometry of the galaxies.

Name	V	$B-V$	$V-R$	H	$J-H$	$H-K$	$V-K$	$L(K)$	$L(\mathrm{H}\alpha)/L(K)$
	(mag)	(mag)	(mag)	(mag)	(mag)	(mag)	(mag)	$\times 10^{43}$ ergs/s/cm^2	
LT41[a]	16.07±0.08	0.88	0.51	13.61±0.10	0.71	0.28	2.74	1.10	0.040
Cartwheel	13.68±0.05	0.35	----	11.72±0.05	0.49	0.17	2.13	5.70	0.049
IIIZw33	14.51±0.05	0.36	0.52	12.78±0.07	0.43	0.43	2.16	2.70	0.018
NGC985[a]	13.57±0.09	0.65	0.41	10.40±0.04	0.23	−0.10	3.07	14.9	0.002
Arp10	13.45±0.07	0.80	0.42	----------	----	----	----	----	----
IIZw28	14.98±0.05	0.32	−0.04	13.44±0.07	0.47	0.34	1.88	1.40	0.020
IIHz4[a]	14.45±0.05	1.22	0.48	12.34±0.06	0.67	0.44	2.55	4.20	0.006
WN1[a]	14.93±0.05	0.71	0.60	12.03±0.08	0.74	0.35	3.25	1.55	0.045
	(15.47)[b]	(0.73)	(0.43)	(12.70)	(1.07)	(−0.26)	(2.51)		
VIIZw466[a]	15.25±0.05	0.33	0.31	13.32±0.13	0.64	0.14	2.07	1.26	0.034
Abell 76	14.73±0.07	0.40	0.29	13.45±0.07	0.51	0.10	1.38	1.10	----
LT36	14.42±0.05	0.66	0.46	12.18±0.05	0.65	0.25	2.49	4.00	0.007

Notes: Optical Data for Cartwheel from Higdon (Private Communication).

[a]Galaxies with significant K-correction applied to data (see text).
[b]Excluding Seyfert nucleus.

colors of some of the rings. However, we note that a decomposition of the light into "bulge" and "ring" is non-trivial in the case of galaxies suspected of being collisional systems, especially when they are observed under conditions of average seeing (1–3 arcsecs). In Sec. 6, we present radial profiles for 4 of the larger galaxy and demonstrate that large radial color gradients are present in most cases. The light distribution is rather complicated in these galaxies, and initial attempts to decompose the light into a disk and bulge were not successful (see one of the few successes, NGC 985—Appleton & Marcum 1993).

Aside from the problem of poor angular resolution, there are reasons to be cautious about oversimplifying the decomposition of the light into "bulge," "disk," and "ring." If, as we suspect, the majority of our ring sample are collisionally induced rings, created by the mechanism discussed by Lynds & Toomre (1976), then light at radii interior to the outer ring can come from at least two different sources: (a) from a pre-existing bulge (a bulge already in existence before the head-on collision), (b) an increased concentration of mainly disk stars in the inner regions due to the ring formation process. This latter component could contain both old disk stars (present before the collision but redistributed by the gravitational perturbation) and a newly produced "young" stellar population formed in the wake of the expanding ring. Indeed it has been argued that much of the light inside the ring of the Cartwheel (Marcum *et al.* 1992) is dominated by newly formed stars. An additional complication is the confusing effects of additional rings in the inner regions. In the case of Arp 10, a blue ring is clearly resolved in the nuclear regions (Sec. 6). The decomposition of these possible components is difficult (and probably quite arbitrary). We have therefore decided to adopt a conservative approach of simply isolating the outer ring light from the "interior" light to gain a first-order impression of the contribution from the inner regions. In some cases, this interior component is dominated by a bulge, but in other cases, this is not the case.

Because of the above considerations, we therefore have adopted the simplest possible separation between ring and ring galaxy. These data are presented in Tables 2 and 3. The format for Tables 2 and 3 is quite similar except that Table 2 is for total ring light, and Table 3 represents data which includes only the emission from the outer ring of the ring galaxy. In all cases, care was taken to exclude any known foreground stars (for example a foreground star is observed within the ring of II Hz 4). Column 1 gives the name of the galaxy. Columns 2–4 present the V, $B-V$, and $V-R$ optical

TABLE 3. Optical and IR photometry of the outer ring component.

Name	V	$B-V$	$V-R$	H	$J-H$	$H-K$	$V-K$
	(mag)	(mag)	(mag)	(mag)	(mag)	mag)	(mag)
LT41	16.60±0.1	0.76	0.44	14.33±0.15	0.74	0.28	2.58
Cartwheel	----	0.23[a]	----	----------	----	----	1.41[a]
IIIZw33	16.24±0.1	0.30	0.52	14.70±0.15	0.44	0.26	1.80
NGC985	14.44±0.1	0.73	0.31	----------	0.8[b]	0.1[b]	----
Arp10	14.85±0.1	0.69	0.33	----------	----	----	----
IIZw28	16.65±0.1	0.52	0.00	13.64±0.15	0.48	0.33	3.34
IIHz4	16.31±0.1	0.46	0.18	13.46±0.1	0.98	0.09	2.94
WN1	16.19±0.1	0.60	0.59	13.38±0.1	0.72	0.18	2.99
VIIZw466	15.12±0.1	0.3	0.13	13.56±0.1	0.6	0.26	1.82
Abell 76	15.18±0.1	0.41	0.27	14.04±0.15	0.49	0.1	1.24
LT36	15.18±0.1	0.58	0.41	13.3 ±0.1	0.62	0.24	2.15

[a]Colors from Marcum *et al.* (1992).
[b]Average ring color from Appleton & Marcum (1994).

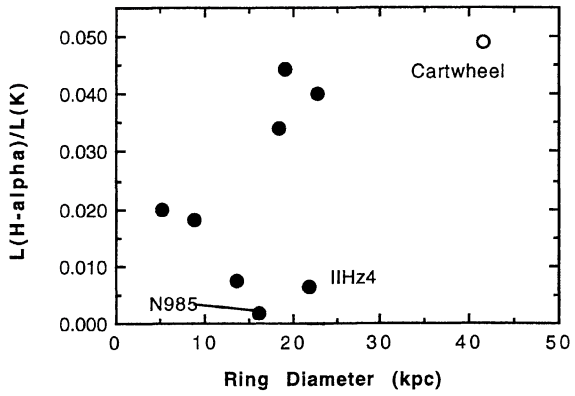

FIG. 12. The ratio of the Hα to K-band luminosity of the galaxies plotted against the linear diameter of the rings.

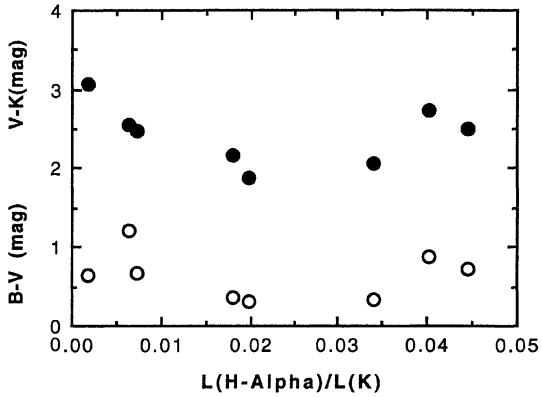

FIG. 13. The $B-V$ and $V-K$ colors of the rings plotted against the ration of L(Hα)/L(K). The latter quantity may be taken as an indicator of the strength of current star formation in the galaxy, and this seems uncorrelated with the global color of the galaxy.

magnitudes and columns 5–7 provides the infrared magnitudes and colors. H, $J-H$, and $H-K$. Column 8 presents the $V-K$ color. These data has been corrected for Galactic extinction using values of extinction estimated from the E(B-V) maps of the Galaxy presented Burstein & Heiles (1982). The conversion of E($B-V$) to extinction in the various bands assumes a standard form for the interstellar extinction law. In most cases the extinction was small (i.e., Av less than 0.2) with the exception of two galaxies, II Zw 28 (A_v=0.26), Abell 76 (A_v=0.29). The galaxies have also been corrected for the effects of redshift via the K-correction (optical corrections from Pence (1976) and IR corrections from Thuan & Puschell (1989)). In four cases, LT 41, VII Zw 466, II Hz 4, and NGC 985 the corrections were significant. For the Seyfert galaxy WN1, we show in Table 2, the magnitudes and colors for the galaxy with and without the bright Seyfert core.

The CCD observations support the early work that collisional ring galaxies are generally blue objects. We note that since the early photoelectric aperture-photometry of Theys & Spiegel (1976), who observed four ring galaxies at $U-B$ and $B-V$, very little work has been done on ring galaxies with the exception of a few scattered individual examples (Few & Madore 1986, AM 064−741; Thompson & Theys 1978, VII Zw 466; Higdon 1993, Cartwheel; and Wallin & Struck-Marcell 1994, AM 1724−622). Taking the galaxies as a whole (i.e., including the interior light as well as the ring) the median and mean values of $B-V$ in our sample are 0.65 and 0.60, respectively, and the median and mean $V-K$ colors are 2.33 and 2.37, respectively. However a very large range in color is observed. The bluest ring is II Zw 28 ($B-V=0.32$) and the reddest ring is II Hz 4 ($B-V=1.22$).

Column 9 of Table 2 shows the K-band luminosities of the galaxies after they have been K-corrected according to their redshifts. Column 10 shows the ratio of the Hα luminosity to the K-band luminosity, L(Hα)/L(K). The values of L(Hα) are taken from MA. This represents a rough measure of the ratio of the current star formation rate to the mass in old stars (assuming that the K-band flux represents mainly an old stellar population). In Fig. 12 we present the ratio L(Hα)/L(K) as a function of the ring diameter. Although the statistics are poor, the plot shows that the Cartwheel, though significantly more luminous in its Hα emission than the other galaxies (see MA) has a ratio of L(Hα)/L(K) which is only a little higher than three of the other larger rings. Interestingly, two of the large classical rings (II Hz 4 and NGC 985) show low values of L(Hα)/L(K). For NGC 985, the low value of L(Hα)/L(K) is most likely explained by significant additional light at K-band from the embedded companion (see Appleton & Marcum 1993). Unlike the other rings, II Hz 4 appears to be heavily dominated by an older stellar population, a result supported by its unusually red $B-V$ color (note however that the ring is blue—see Table 3). No clear trend of L(Hα)/L(K) with diameter of the ring emerges. Such a trend might have been expected if the efficiency of star formation increased as the ring wave developed (as for example in some of the models of Appleton & Struck-Marcell (1987b)).

The ratio L(Hα)/L(K) for the ring galaxies is also plotted against both $B-V$ and $V-K$ color in Fig. 13. The plot shows that the global colors of the galaxy (as measured by both optical and optical-IR baselines) are independent of the present day star formation rate per unit galaxy luminosity.

TABLE 4. Companions to ring galaxies.

Name	V	$B-V$	$V-R$	H	$J-H$	$H-K$	$V-K$
	(mag)	(mag)	(mag)	(mag)	(mag)	(mag)	(mag)
LT41b	16.40±0.08	1.30	0.64	13.68±0.10	0.67	0.24	2.96
IIHz4b	15.88±0.05	1.83	0.58	13.87±0.06	0.98	0.17	2.18
WN1b	16.10±0.05	0.95	0.68	12.65±0.08	0.75	0.30	3.75
VIIZw466G1 (Ellip)	15.96±0.05	0.73	0.34	----------	----	----	----
VIIZw466G2 (Sp)	15.04±0.05	1.12	0.40	----------	----	----	----

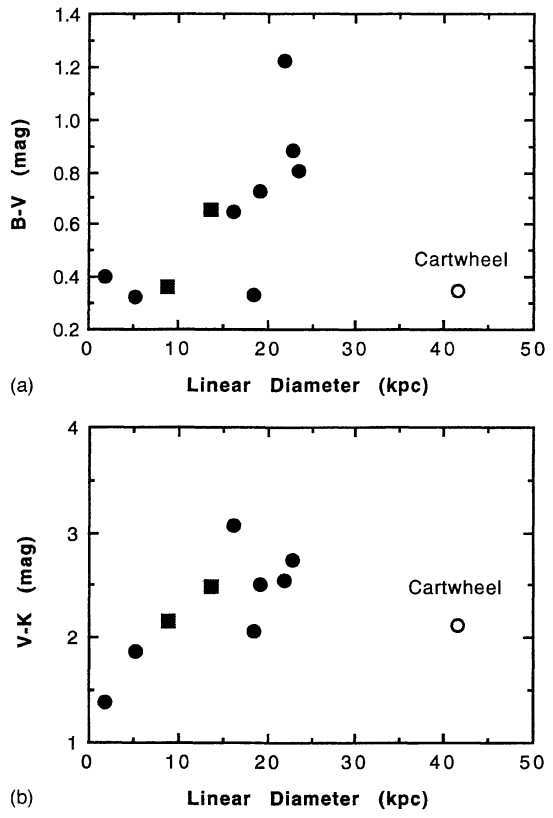

FIG. 14. Ring diameters vs (a) $B-V$, (b) $V-K$ color for the ring galaxies. The Cartwheel ring is shown as an open circle and the two less classical rings are shown as squares. The other galaxies are shown as filled circles.

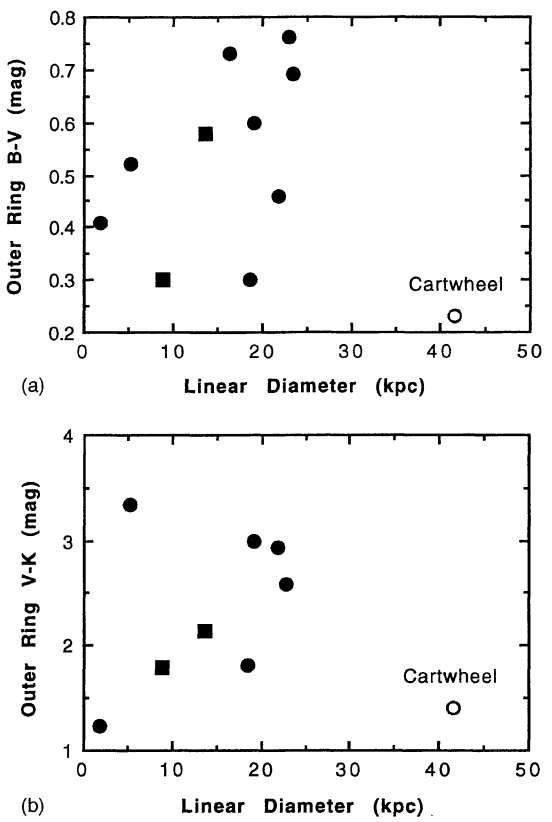

FIG. 15. (a) and (b) same as Fig. 14 but colors represent the outer ring emission only (see text).

This conclusion is based on the lack of any obvious trend of color with L(Hα)/L(K). For example galaxies with high current rates of star formation per unit K-band luminosity are not significantly bluer than those with low SFRs/unit luminosity.

In Figs. 14(a) and 14(b) we show the $B-V$ and $V-K$ colors, respectively, of the ring galaxies as a function of the linear ring diameter. For the integrated light (Fig. 14), there is a tendency for smaller rings to have bluer colors, whereas the larger rings (with the exception of the Cartwheel) have a larger spread in colors with a mean value that is redder than the small rings. The galaxy II Hz 4 is the reddest galaxy in the sample in global $B-V$ color. In $V-K$ color, II Hz 4 would be the reddest, except for the two Seyfert rings, WN1 and NGC 985. Despite the removal of a red point-like core in the Seyfert galaxy WN1, this galaxy, and NGC 985 have the reddest $V-K$ colors of the rings in this sample. We note that the Cartwheel, which has the largest linear diameter of the rings in this sample is one of the bluest galaxies in $B-V$ color, although its $V-K$ color is average for the sample.

Figures 15(a) and 15(b) are similar to those of Fig. 14, but for the outer ring light only (i.e., excluding the ring interior). The overall spread in $B-V$ and $V-K$ color is significantly less than those in Fig. 14. For example, for the global light, the spread in $B-V$ is over 1 mag for the sample, but for the outer rings alone, this drops to approximately 0.5 mag. Interestingly, this effect is largest for the largest rings. With the exception of II Zw 28,[2] most of the small rings did not change significantly in color when the interiors were excluded. However, the largest rings show the most significant change, and this is undoubtedly due to the existence of red nuclei or bulges in these cases. This is confirmed by studying the radial profiles shown in Sec. 6.

One general conclusion that can be drawn from the above analysis is that the possible trend of $V-K$ color with radius seen in Fig. 14(b), is probably due to a tendency of larger ring galaxies to contain red bulges or nuclei. The result is tantalizing, since the numbers of ring galaxies are very small in the sample. A number of effects could contribute to the increased redness of the larger ring centers. These include, (a) the existence of active nuclei in two of the galaxies (NGC 985 and WN1), (b) an increase in both the number of evolved stars in the center as a result of the dynamics of the ring-making collisions, (c) enhanced concentration of dust in the nuclear regions due to infall and collapse of gas behind the ring. (Dust filaments are seen in the Cartwheel *HST* observations, see Struck *et al.* 1996), (d) some form of selection effect which might cause an increased frequency of bulge-dominated rings when the rings are large.

In order to remind the reader that the sample is small, we

[2]II Zw 28 showed an increase in $V-K$ color when the interior of the ring was excluded. This we believe is due to the existence of a very bright red component embedded in the ring. This may either be an off-center nucleus, or the companion seen in projection against the ring.

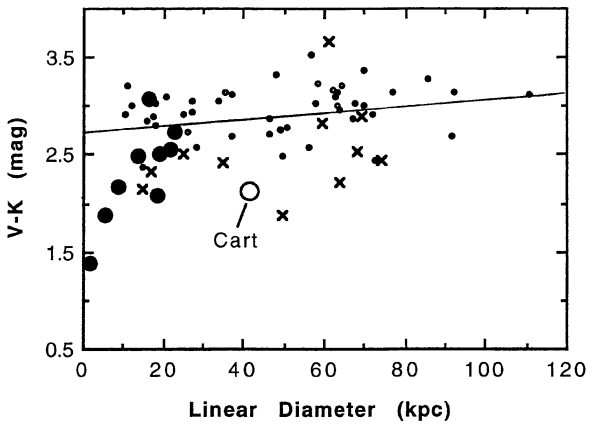

FIG. 16. The $V-K$ color of the rings versus linear diameter (solid circles), Cartwheel ring (open circle) and the spiral galaxies of De Jong (1995). The spiral sample is coded according to Hubble type (late type spirals: crosses, intermediate types: solid circles (small) and early types: open circles (small). The line is the least-squares fit to the entire De Jong sample.

finally show the possible trend of $V-K$ color with ring size (discussed above) in context with a major study of spiral galaxies made by de Jong (1995). Figure 16 shows the $V-K$ color of 89 spiral galaxies taken from de Jong's UGC galaxy survey plotted against their linear diameters assuming a Hubble constant of 75 km s^{-1} Mpc^{-1}. The diameters of the spiral sample are taken from the UGC Catalog (Nilsen 1973) and would seem to be comparable with the ring diameters, because the ring light falls sharply outside the rings and provided a sharp cut-off to the isophotal size. The de Jong galaxies are shown as small symbols (coded according to Hubble type) and the large filled dots represent the colors of the current ring sample. The solid line represents a least squares fit to the de Jong data, showing a slight tendency for larger galaxies to be redder than smaller galaxies, but this is a smaller effect than that seen in the rings. However, significant scatter is seen in both samples. Much of the scatter in the spiral sample is due to the Hubble-type dependence of the colors. For the intermediate Hubble types ($T = 2-4$) the scatter is small and the correlation is quite good. The late-type galaxies show a larger scatter however, and the spread in their over-all colors is quite similar to the spread in the $V-K$ colors of the rings. Ideally, many more ring galaxies would be needed to unambiguously determine whether the trend of color with radius is real, or just a result of small number statistics.

In Table 4 we present photometry for companion galaxies to the ring systems. Only those galaxies that are very likely to be companions are included in the table. These data have been reduced in the same way as in Table 2. The main result from the companion study is that in all cases the companion is redder than the associated ring galaxy.

6. RADIAL PROFILES FOR THE LARGER GALAXIES

In this section was have selected four of the larger galaxies (VII Zw 466, Arp 10, LT 41, and II HZ 4) for a detailed study of their radial luminosity and color profiles. In the Cartwheel galaxy MAH showed that large color gradients

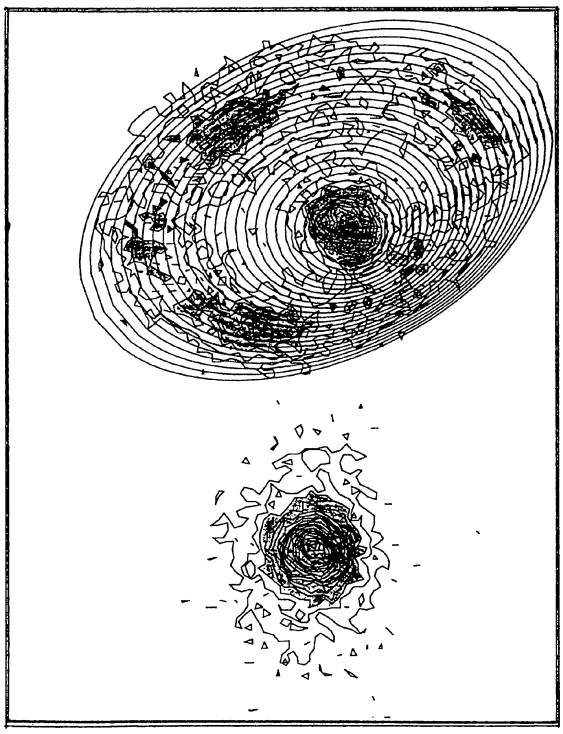

FIG. 17. Schematic representation of the nested ring method for determining the radial surface brightness of a galaxy with an offcenter nucleus (see text). This example is for LT 41.

existed in the galaxy consistent with stellar evolution behind the expanding wave. With the exception of VII Zw 466, the other three galaxies shown here contain complicating nuclear bulges making the interpretation of the colors more difficult. We will restrict ourselves here to presenting these data and determining the overall properties of the systems. In a later paper we will discuss the color gradients in the context of various models.

The determination of the azimuthally averaged radial light distribution in galaxies with off-centered nuclei is non-trivial. We adopted the approach that our radial profiles should in some way take into account the fact that the center of the outer ring is often not coincident with the center of the inner nucleus. The radial distributions were determined as follows. The optical images were first smoothed to the slightly lower spatial resolution of the IR images to ensure that the colors were evaluated over similar spatial regions. Then two centers were determined for each galaxy. The first center was chosen to be the center of the nucleus, if present. The second center was chosen to be the center of the outer ring (the point of intersection between the major and minor axes). Since II Hz 4, LT 41, and Arp 10 all have offcenter nuclei, these two centers were not, in general, the same. A series of nested elliptical annular rings were then constructed of fixed width, but of increasing dimensions. The inner elliptical rings were initially centered on the nucleus, but as the radius was increased, the center of each subsequent ellipse was shifted slightly, so that as the ellipse reached the size of the outer ring, the center would have moved to the outer ring center. In addition, the ellipticity of the ellipses was also

allowed to smoothly change from the inner to the outer regions, reflecting changes in shape between the outer ring and the often circular nucleus. An example of this form of sampling is shown in Fig. 17 for the case of LT 41. Count rates were then determined within each successive annular ring and these were converted into surface brightness ratios. The K-band images were re-gridded onto the same spatial grid as the optical data before the calculation was performed. Careful checks were made to ensure flux conservation in this latter process. The major axis dimension of each ellipse was then taken to be the "radius" of the ellipse in the radial distributions shown here. These would correspond to true projected radii if the rings were circles seen inclined to the line of sight.

In Figs. 18(a), 18(b) to 21(a), 21(b) we present the radial surface-brightness profiles for each of the four galaxies. In each case the B, R, and K-band surface brightness profiles (part (a) of the figure)and the $B-R$, $R-K$, and $B-K$ colors are shown (part (b) of the figures).

The radial profiles for II Hz 4, LT 41, and Arp 10 (Figs. 18(a), 19(a), 20(a)) show very similar behavior, with a central steep fall away from the nucleus, followed by a broader rise to the ring and then a fall-off outside of the ring. In most cases the contrast between the outer ring and the intermediate region (between nucleus and ring) is much higher at B than at R and K. At K-band the ring is more filled in and inside the ring the emission is almost of constant surface brightness. This implies a color gradient on the inside edge of the ring and indeed in most cases such a gradient is seen. In II Hz 4 (Fig. 18(b)), the $B-V$ color falls slowly at first but increases across the ring in the outer regions. Notice very little indication of a major increase in reddening in the nuclear regions. Such flat color distributions have been noted by de Jong (1995) in his sample of ordinary spiral galaxies. In the outer regions, the galaxy becomes redder again. However, we caution that in this system, spill-over light from the bright nearby star may be a concern at low levels. However, a similar effect is seen in VII Zw 466 (below) and the Cartwheel (Appleton *et al.* in preparation) and so it may be a real effect. LT 41 (Fig. 19(b)) shows a very constant gradient in color from the inner bulge to the outer ring, with very little change in slope across the entire galaxy. Overall, the color changes from center to outer ring are pretty featureless in this galaxy. The $B-K$ change from nucleus to outer ring is about 1.5 magnitudes. Arp 10 (Fig. 20(b)) shows the most interesting fine structure in the color distributions. Because of the large angular size of Arp 10, no K-band data was obtained for the entire ring and so no IR color information is available. However, at a radius of a few arcsecs, the inner blue star forming ring becomes very obvious as a sudden drop in $B-R$ color (Hα emission is seen in this ring, see Charmandaris *et al.* 1993). Also, in the outer ring, sudden changes in color are observed across the ring, first a blueward swing on the inside edge of the ring, and then a reddening on the outer edge. Fine structure of this type is not unexpected in ring galaxies, since second rings may well form in the inner regions if the elapse-time since the collision is long enough. This underlines the need for higher spatial resolution in many of the more distant ring systems in order to ensure that all the possible components of the system are recognized.

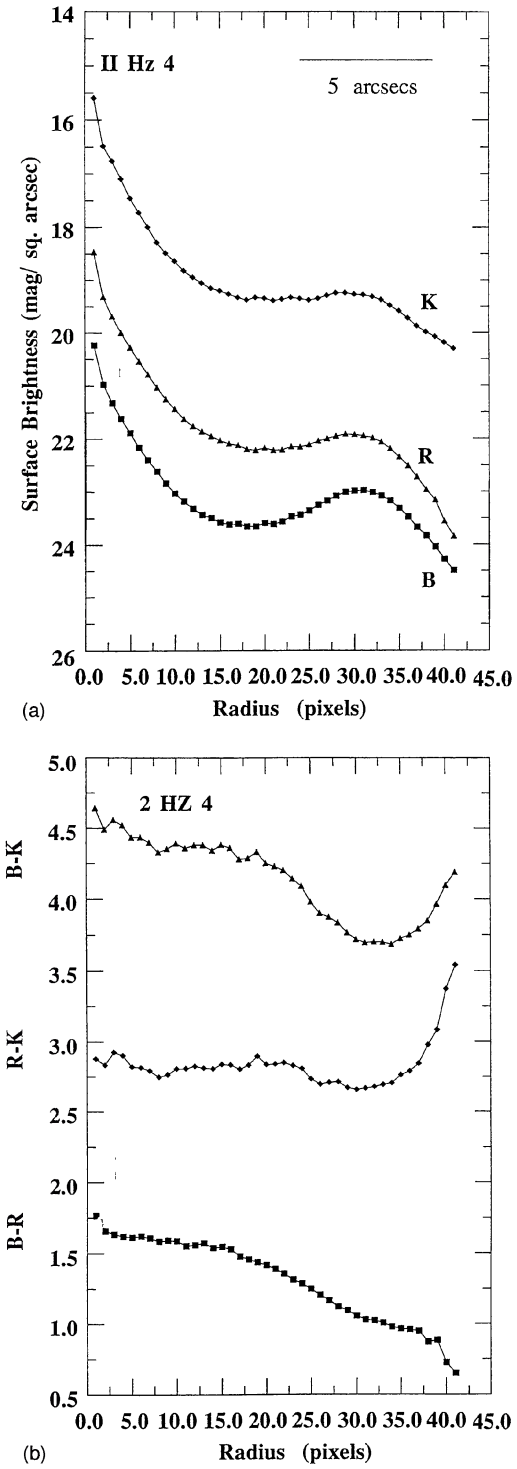

FIG. 18. (a) Radial surface brightness profile for galaxy II Hz 4, (b) color profiles for II Hz 4.

The most fascinating system of our sample is VII Zw 466. This galaxy lacks a nucleus, and indeed its radial profiles are very different from those of the other rings. Figure 21(a) and 21(b) show the luminosity and color profiles for the galaxy,

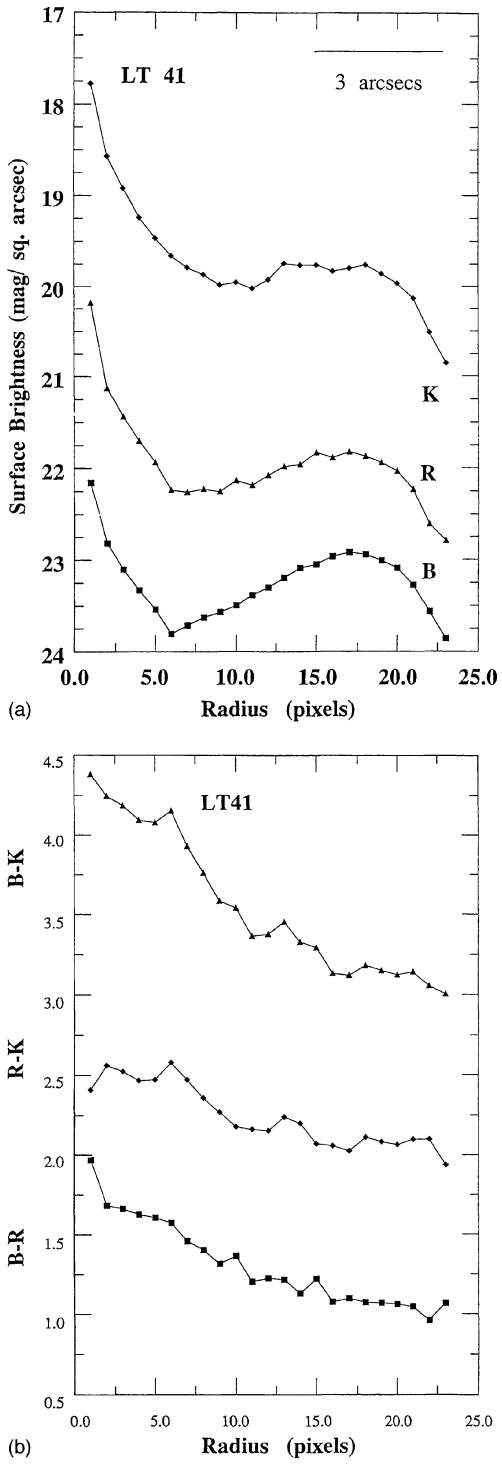

FIG. 19. (a) and (b) as for Fig. 18 but for galaxy LT 41.

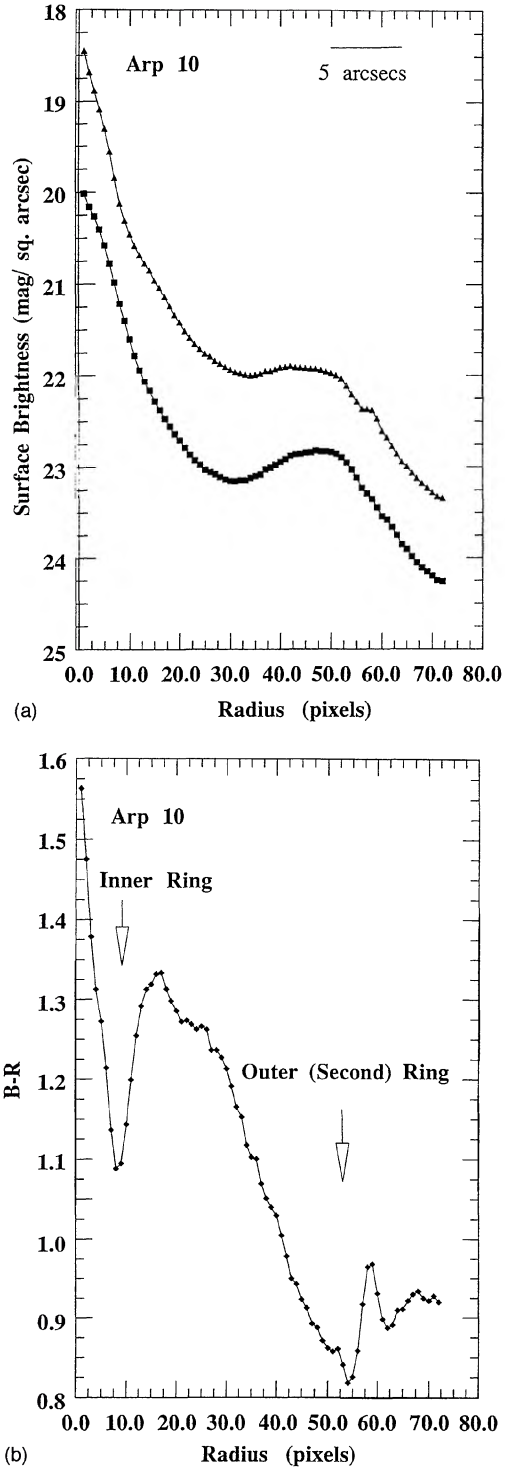

FIG. 20. (a) and (b) as for Fig. 18 but for galaxy Arp 10.

azimuthally averaged around a full 360°. Some structure is seen within the ring, and this is due to the existence of a red knot which lies displaced from the northern edge of the ring (see Sec. *4.3*). The color distribution also shows interesting structure. Red light fills the ring and in $B-R$ the color declines uniformly from the center outwards dropping by about 0.75 mag over the radius of the ring. At about the peak luminosity in the ring, the color reddens again similar to the behavior found in II Hz 4. In the IR bands (reflected especially in the $R-K$ and $B-K$ colors) a bump in the color distribution corresponds to the slightly interior knot.

In order to better explore VII Zw 466, we divided the

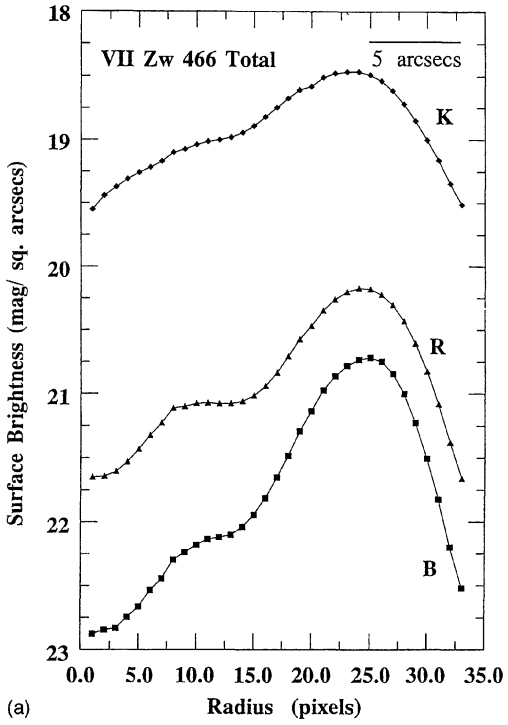

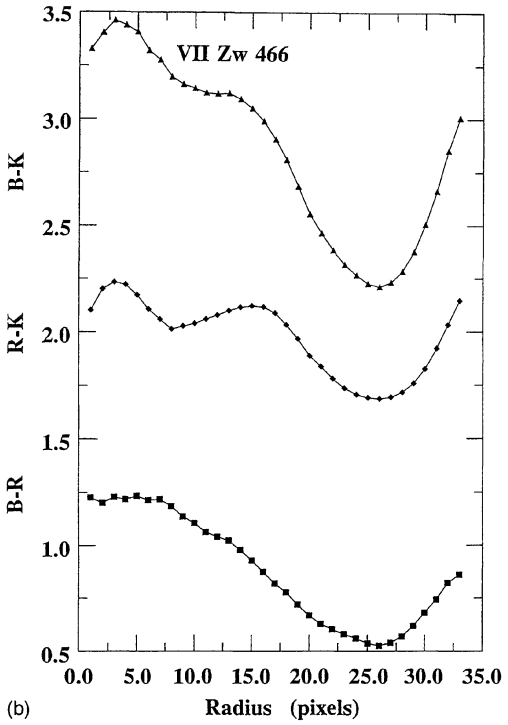

FIG. 21. (a) and (b) as for Fig. 18 but for galaxy VII Zw 466.

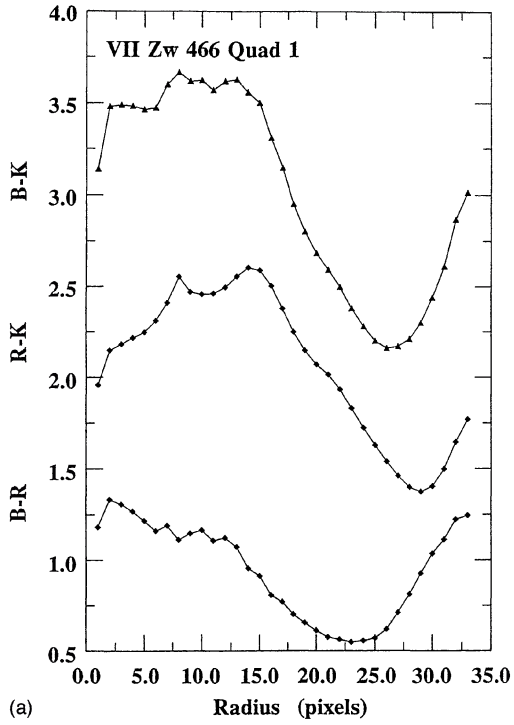

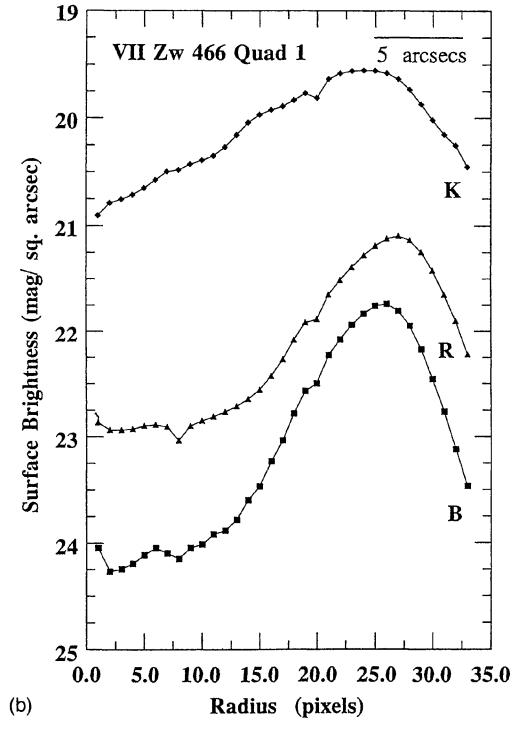

FIG. 22. (a) and (b) as for Fig. 21, but for Quadrant 1 of VII Zw 466.

radial distributions up into 4 quadrants, corresponding to 4 equal segments of the galaxy working counterclockwise from the northern major axis. We determine the P.A. of the major axis to be −30° (n through e). Quadrant 1 covers a P.A. of −30° to +60°. Quadrant 2 covers the P.A. range +60 to +150, and the other two quadrant follow the same pattern. This means that Quadrants 1 and 4 cover the regions of the interior knot, but Quadrants 2 and 3 cover essentially the eastern side of the galaxy, and are free of any interior knots.

Figures 22(a), 22(b) to 25(a), 25(b) show the radial profiles of the four quadrants. As expected Quadrants 1 and 4

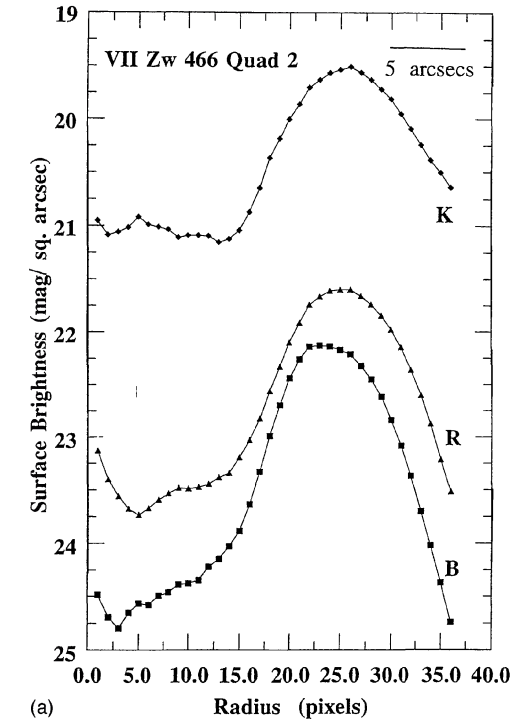

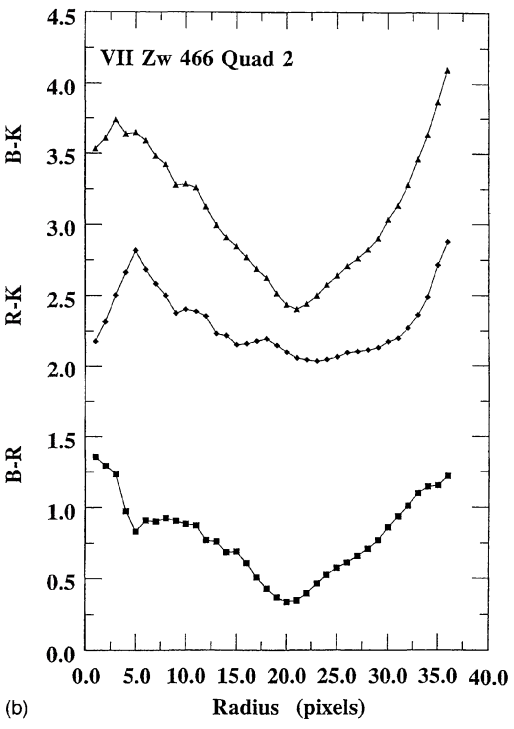

FIG. 23. (a) and (b) as for Fig. 21, but for Quadrant 2 of VII Zw 466.

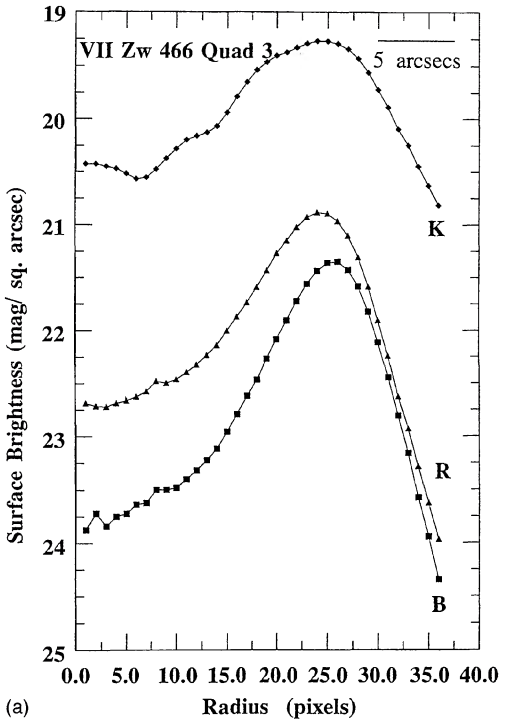

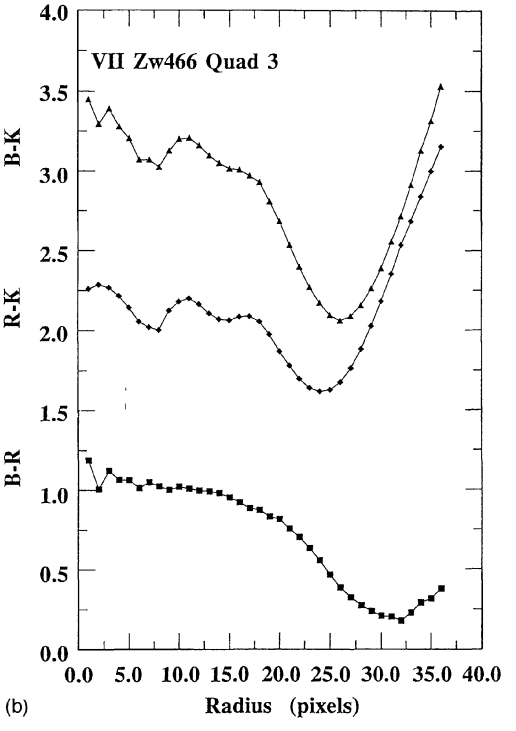

FIG. 24. (a) and (b) as for Fig. 21, but for Quadrant 3 of VII Zw 466.

show the existence of the interior knot. The effect is to flatten the color distributions in the inner regions, but then colors decrease (become bluer) rapidly just as the bright blue ring is encountered. The colors redden again outside this region. Quadrants 2 and 3 show a flat surface brightness profile interior to the ring emission (at about 24–24.5 mag square arcsecs at B), and then a more sudden rise to the eastern edge of the ring. In the inner ring region, the colors in all bands fall (become bluer) constantly to the radius of the ring, and then show an upswing on the outer edge of the ring. The upswing in Quadrant 3 occurs sooner (at smaller radii) in the IR color baselines than in the B-R color. We

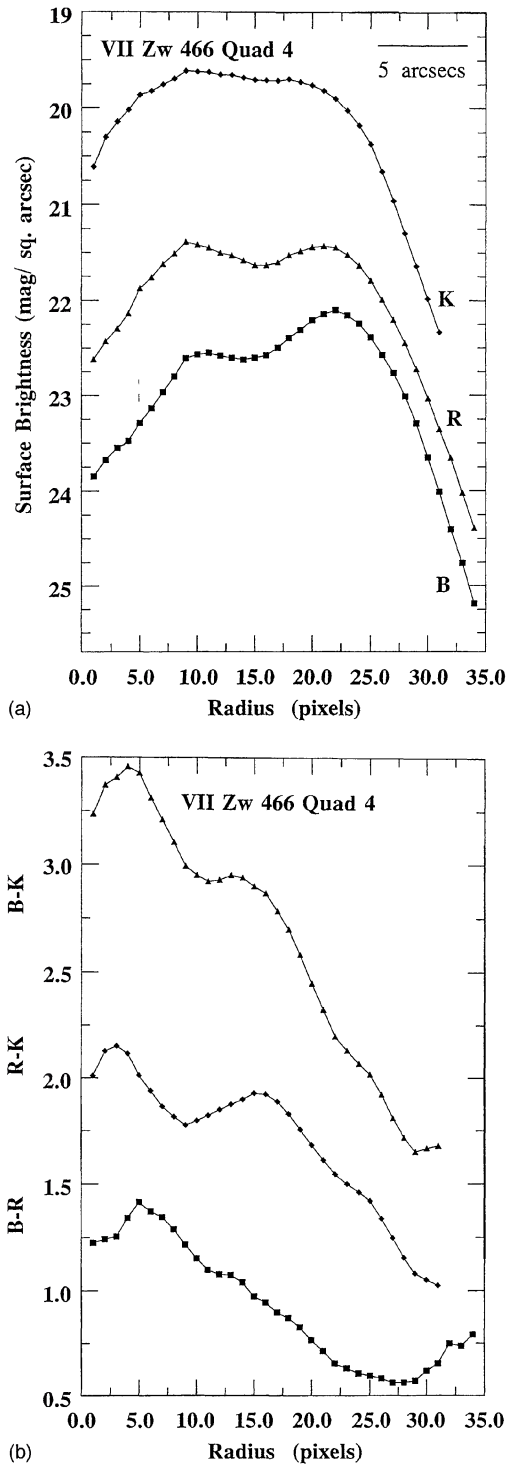

FIG. 25. (a) and (b) as for Fig. 21, but for Quadrant 4 of VII Zw 466.

emphasize that this reddening in the outer edges of the ring is not a signal-to-noise effect, since the color changes begin to occur where the surface brightness is well above the noise-level and the effect appears to be real.

The structure seen in the color distributions of the rings is interesting. The interiors of the rings are red, show a sometimes rapid radial color gradient towards the blue, and in two cases show a reddening in the outer regions, outside the main ring H II regions. Interestingly LT 41 does not show this reddening. One possible explanation for the outer red emission is that, in the collisional picture, the blue star forming ring has not yet propagated to the outer edge of the original target disk and the red light may represent the stellar population of the progenitor galaxy. Presumably either LT 41 was a low surface brightness galaxy before the collision, or its ring has already reached the edge of its stellar disk.

7. CONCLUSIONS

Optical and near-IR imaging is presented of a sample of 11 possible collisional ring galaxies we conclude that:

(1) The near-IR and optical morphologies of a sample of ring galaxies show remarkable similarities. In almost all cases there is a one to one correspondence between the K-band knots and the B-band knots in the rings. A similar result was obtained in earlier studies of the Cartwheel (MAH). This result suggests that the knots are real condensations in the rings and are not simply a result of patchy optical obscuration around the rings. The existence of clumpy star formation regions around the rings supports the idea (Struck-Marcell & Higdon 1993; Hernquist & Weil 1993) that pre-existing overdense regions in the target disk can be amplified by the passing density wave leading to star formation. Such clumpy structure may provide a natural explanation for the later formation of spokes, as in the Cartwheel ring galaxy.

(2) In only one case, the Seyfert ring galaxy WN1 (=Bootes ring) do we observe marked differences in IR to optical morphology. In this case it is the companion galaxy and not the ring that is significantly different. These differences can be explained by the obscuration of the companion by the foreground disk of the ring galaxy.

(3) Radial spokes similar to those seen in the Cartwheel ring galaxy seem to be rare amongst classical ring systems. Only II Hz 4 shows any evidence for radial features connecting the ring to the central regions, and in this case we suspect that the structure may be more akin to a $m=2$ spiral resonance (see, Appleton & James 1990) than the spokes seen in the Cartwheel.

(4) The optical and IR colors or ring galaxies are blue (Median $B-V$ and $V-K$ colors are 0.65, 2.33, respectively). This is consistent with the observation that most of the current star formation is occurring in the rings and not from inside the rings (MA).

(5) There is a suggestion that the global $V-K$ color of the rings increases with the linear diameter of the ring. The effect may be due to an increased fraction of the larger galaxies containing red nuclei or bulges. It is not yet clear if this is a dynamical effect of the collisions (larger rings are likely to be more dynamically evolved than small rings), contamination by dust emission, or if this is a result of some unknown selection effect in the sample.

(6) Radial profiles of total light and color are presented for 4 of the larger galaxies. The rings, whether containing

bulges or not, show an initial steep fall in color from red at the center to blue at the ring, similar to that seen in the Cartwheel galaxy (Marcum *et al.* 1992; Higdon 1993). In two cases, a significant reddening is seen in the regions outside the radius of the main star formation ring, suggesting the existence of an outer (red) disk. Outer red light would be expected in the collisional picture if the outwardly propagating ring wave has not yet reached the edge of the preexisting stellar disk of the target galaxy.

We wish to thank C. Struck for helpful comments on the manuscript. We are grateful for the advice of an anonymous referee who made some helpful suggestions about the presentation of the results. This work is supported by NSF Grant No. AST-9319596.

REFERENCES

Appleton, P. N., Charmandaris, V., & Struck, C. 1996, ApJ, 468, 532
Appleton, P. N., Kawaler, S. D., & Eitter, J. J. 1993, AJ, 106, 1973
Appleton, P. N., & James, R. A. 1990, in Dynamics and Interactions of Galaxies, edited by R. Wielen (Springer, Berlin), p. 200
Appleton, P. N., & Marcum, P. M. 1993, ApJ, 417, 90
Appleton, P. N., Robson, E. I., & Schombert, J. M. 1990, in Paired and Interacting Galaxies, Proc. of IAU Colloquium No. 124 (NASA Conf. Publ. No. 3098), p. 59
Appleton, P. N., Schombert, J. M., & Robson, E. I. 1992, ApJ, 385, 491
Appleton, P. N., & Struck-Marcell, C. 1987a, ApJ, 312, 566
Appleton, P. N., & Struck-Marcell, C. 1987b, ApJ, 318, 103
Appleton, P. N., & Struck-Marcell, C. 1996, Fund. Cosm. Phys., 16, 111
Arp, H. C., & Madore, B. F. 1987, Catalog of Southern Peculiar Galaxies and Associations, Vols. I & II (Cambridge University Press, Cambridge, UK)
Athanassoula, E., & Bosma, A. 1985, ARA&A, 23, 147
Burstein, D., & Heiles, C. 1982, AJ, 87, 1165
Bushouse, H., & Stanford, S. A. 1992, ApJS, 79, 213
Buta, R. J. 1986, ApJS, 61, 609
Cannon, R. D. Loyd, C. & Penston, M. V. 1970, Observatory, 90, 153
Charmandaris, V., & Appleton, P. N. 1996, ApJ, 460, 686
Charmandaris, V., Appleton, P. N., & Marston, A. P. 1993, ApJ, 414, 154 (CAM)
De Jong, R. S. 1995, Ph.D. thesis, University of Groningen, Netherlands
Elias, J. H., Frogel, J. A., Matthews, K., & Neugebaur, G. 1982, AJ, 87, 1029
Few, J. M. A., & Madore, B. F. 1986, MNRAS, 222, 673
Fosbury, R. A. E., & Hawaden, T. G. 1977, MNRAS, 178, 473
Gerber, R. A., & Lamb, S. A. 1994, ApJ, 431, 604
Hernquist, L., & Weil, M. L. 1993, MNRAS, 261, 804
Higdon, J. L. 1993, Ph.D. thesis, University of Texas at Austin
Horellou, C., Casoli, F., Combes, F., & Dupraz, C. 1995, A&A, 298, 743
Jeske, N. 1986, Ph.D. thesis, University of California at Berkeley
Landolt, A. U. 1992, ApJ, 104, 340
Lynds, R., & Toomre, A. 1976, ApJ, 209, 382
Marcum, P. M., Appleton, P. N., & Higdon, J. L. 1992, ApJ, 399, 57 (MAH)
Marston, A. P., & Appleton, P. N. 1995, AJ, 109, 1002 (Paper I=MA)
Mazzei, P., Curir, A., & Bonoli, C. 1995, AJ, 110, 559
McCain, C. 1996, Ph.D. thesis, Australia National University, Canberra
Nilsen, P. 1973, Uppsala General Catalogue of Galaxies (Royal Society of Sciences, Uppsala, Sweden)
Pence, W. 1976, ApJ, 203, 39
Rodriquez-Espinosa, J. M., & Stanga, R. M. 1990, ApJ, 365, 502
Sargent, W. L. W. 1977 ApJ, 160, 405
Schultz, A. B., Spight, L. D., Colegrove, P. T., & Di Santi, M. A. 1990, Massive Stars in Starbursts (STScI Workshop, Baltimore)
Struck-Marcell, C. 1990, AJ, 99, 71
Struck-Marcell, C., & Higdon, J. L. 1993, ApJ, 411, 108
Struck, C., Appleton, P. N., Borne, K., & Lucas, R. 1996, AJ, 112, 1868
Talent, D. L., Kaler, J. B., Gallagher, J. S., & Hunter, D. A. 1982, ApJ, 260, 488
Theys, J. C., & Spiegel, E. A. 1976, ApJ, 208, 650
Thompson, L. A. 1977, ApJ, 211, 684
Thompson, L. A., & Theys, J. C. 1978, ApJ, 224, 796
Thuan, T. X., & Puschell, J. I. 1989, ApJ, 346, 34
Toomre, A. 1978, in The Large Scale Structure of the Universe, IAU Symposium 79, edited by M. S. Longair and J. Einasto (Reidel, Netherlands), p. 109
Wakamatsu, K., & Nishida, M. T. 1987, ApJ, 315, L2
Wallin, J. F., & Struck-Marcell, C. 1994, ApJ, 433, 631
Whitmore, B. C., Schweizer, Leither, C., Borne, K., & Roberts, C. 1993, AJ, 106, 1354